

Developing a small scale tool switching mechanism for agricultural integration

Floris Belle

5397839

f.m.belle@student.tudelft.nl

Fedde Jorritsma

5339243

f.b.jorritsma@student.tudelft.nl

Jasper Welgemoed

5411467

j.t.welgemoed@student.tudelft.nl

Kelvin Zwarthoed

5313546

c.t.j.m.zwarthoed@student.tudelft.nl

Abstract—The field of robotics is rapidly growing and expanding, and robotic arms play an important role. An important extension is the development of tool-changing mechanisms. Although there are quite a few solutions for large-scale industrial robotic arms already, there aren't as many options for smaller applications. In the development of small and cheap robot arms, accuracy and repeatability differ greatly from the larger and more expensive counterparts. The aim of this paper is to design a tool-switching mechanism capable of coping with the inaccuracies of small-scale cheap robotic arms. A testsetup including a robotic arm was built and tested and various solutions for a tool-switching mechanism are tested and compared. After building the final design, tests showed a repeatability rate up to 83,1% and a success rate of 98,1%, when allowing for minor errors. These results demonstrate a successful tool-switching mechanism, and further research into its integration in greenhouses is recommended.

I. INTRODUCTION

Traditionally, the Netherlands has had a significant agricultural industry, which is crucial both economically and culturally for the country. Our progressiveness and innovation in this sector, the last 100 years, have made us the second-largest exporter in the world [10]. Due to these innovations, the landscape is continuously evolving and will continue this trend in the upcoming years. These innovations are, now more than ever, necessary to address emerging challenges such as maintaining soil fertility, restoring biodiversity, adhering to the climate agreement, reducing nitrogen emissions, improving animal welfare and labor shortages. Particularly, the labor shortage is a major challenge for greenhouse owners [11]. Therefore, the department of Cognitive Robotics of the TU Delft is currently developing a series of agricultural robots aimed at collaborating with greenhouse workers to address this aspect of labor shortage. The series of robots will primarily consist of iterations on TU Delft's latest platform, the Mirte Master, and will be intended for owners of smaller sized greenhouses. This project will be an iteration on the Mirte Master that is focused on solving the robot's lack of ability to operate multiple tools. Therefore the goal of this project is to design a system which allows the robot to operate and switch between a set of tools stored on the Mirte Master. This project is a continuation of a BEP project from last year. The aim of this

project is to continue the work on this project and improve the performance significantly.

Future iterations of the robot will operate in a greenhouse and must endure challenging conditions such as exposure to dirt, plant debris, high humidity levels, increased temperatures and potential chemical threats that could damage the system. To achieve a fully-fledged final design, the project has been split up in different phases. Each phase has a different primary objective and the culmination of these phases ensure the delivery of a functional end product.

This design research project was being carried out by Mechanical Engineering students from Delft University of Technology.

II. METHODOLOGY

Approaching this project systematically is crucial for successfully completing its main goal. A NASA systems engineering approach has been followed to ensure proper integration between all system components from our own research group and the parallel BEP group 10 [7]. On top of that, a NASA project management approach has been implemented for seamless collaboration within the team and with group 10. As a result, a distinction has been made between seven project phases that each have their own deliverables and decision points. During all seven phases, documentation will be carried out on the project's progress. An overview of these project phases and a top-level project planning is provided in Appendix A.

A. Pre-Phase A - Mission Study

The purpose of pre-phase A is to perform an orientation of different project objectives. Here, the stakeholders are defined and this is done in parallel with an extensive client/stakeholder research that narrows down the solution space such that the project scope can be defined. From this research, stakeholder requirements are discovered that will guide us through the project. The deliverable of this phase is a strong mission need statement that summarizes the client's needs and the goals of the project group into one sentence. This statement will guide the entire project to success. This will be determined in the first week of the project.

B. Phase A - Concept Development

The next phase is the concept development phase. A system definition will first be provided, which includes a description of all the top-level systems and design parameters that need to be taken into account. Primarily, the design from the previous BEP group will be thoroughly analysed for oversights, easy fixes and major design flaws. The results of this analysis will be combined with the stakeholder requirements and our personal project goals, to come up with system-level requirements that will describe the functional-requirements, design-requirements and performance-requirements of the system. Next, concepts for each of the relevant systems will be developed and traded-off against design criteria to narrow down the solution space to about 2/3 concepts per sub-system. The deliverable of this phase is a baseline of the system requirements, a system definition and a preliminary idea of the solution. Together with the supervisors, the requirements and direction of the solution will be validated before continuing to the next phase. This phase will be finished in one week after the closure of Pre-Phase A.

C. Phase B - Preliminary Design

The purpose of Phase B is to narrow down the different concepts from Phase A into a single concept that meets all of the functional requirements. This will be done by performing a final trade-off. After which first-order sizing can be performed and the first prototypes can be created to test the principles of the concept. A 3D-printer will be used for this prototyping stage. This phase is closed-out by reviewing the final concept with the supervisors to get a green light for the detailed design phase. This phase will take 1.5 weeks to finish.

D. Phase C - Detailed-Design

The purpose of this phase is to freeze the solution space to one final solution. After the closure of this phase, the design should be detailed enough to immediately start manufacturing. All the SolidWorks models and finite element analysis should be finished. All connections, software and sub-systems should be fully defined such that a manufacturing plan can be delivered. This phase will be finished within 2 weeks after the end of phase B.

E. Phase D/E - Production/Testing/Final iteration

The purpose of phase D is to perform the production plan and start the full integration between the solution and the solution of the parallel group. Test-plans will be set-up and performed that will validate and verify the performance requirements of the system. Test-reports are the major deliverable of this phase, which will be a large part of the paper. Tests on our system will be used to decide and freeze the final dimensions of the parts. A data analysis will be documented in the report, on which the performance of the system will be analysed. This phase will take one week to finish.

F. Phase F

A final compliance check on all of the requirements will be done with the supervisors to determine the success of the project. Then all the documented work will be gathered and sorted into a proper paper format which will be the final deliverable on the 14th of June.

III. PROJECT SCOPE & SYSTEM DEFINITION

The scope of the project is primarily defined by the needs of the clients, supervisors and any other third party that was involved in the project, but boundaries will be set up by our own constraints such as time, money, resources and personal goals. These will form the scope of our project and will help managing our resources.

A. Supervisors

For supervisors it is important that the system is designed for the agricultural sector and especially for owners of smaller greenhouses. This means the robot needs to be small-scale and affordable. Also they would like to see the design to be easily scalable such that the design can be used for different size greenhouses each with different needs. As well as easily maintainable and manufacturable such that the design can be used during a robotics master course at the TU Delft.

B. Clients

Multiple small greenhouses have been visited in Delfland to talk about the project and to find out the needs of people working in these greenhouses. Questionnaires of these visits are shown in appendix H. The owners mainly want the robot to be affordable which will be taken into the scope as this is also a need of the supervisors. The workers primarily want the robot to be able to recognize and remove weeds through AI. This will be left out of the scope as this requires more advanced programming of robot which is not in our mission need statement. Any other wishes of tool functionalities are left out of the scope as there is another group researching these tools.

C. Environment

The system needs to operate under greenhouse conditions. These conditions first need to be defined and later, tested on our system. Within the scope lies the temperature range, humidity levels and dirt. From the client research (Appendix H) it was concluded that some smaller agriculture companies do not make use of chemicals. Either because of personal believes or governmental restrictions. In consultation, chemical effects and UV resistance have been left out of the scope and will only be discussed during the material selection of our design.

D. Mirte Master

The project is built upon an existing robot called "Mirte Master" that is developed in-house at the TU Delft. Within the scope lies adapting our design to the dimensions and range of motion of the Mirte Master as well as the programming of the

servo motors of the arm to certain coordinates. Any further programming or hardware changes to the Mirte Master fall outside of the project scope.

E. Parallel Research Group

The parallel BEP group, which is conducting research on the tools to be connected to the tool-switching system, have their own requirements that must be met. In order to integrate these two projects into one functional tool switching system, close communication with the other group must be maintained. Within the scope of our project are any geometrical constraints they impose on us, as well as establishing the electrical connection from their tools to the Mirte Master. However, the programming involved in operating their tools, along with the design choices and the type of tools they decide to develop, fall outside the scope of our project.

F. System Definition

Using the scope as a guideline, the system to be designed can be defined with the following components and actions.

- **Bracket** The connection between the end-effector of the Mirte Master's arm to and the robot arm adapter.
- **Robot(ic) Arm Adapter** The interface between the bracket of the Mirte Master's arm and the tool adapter.
- **Tool Adapter** The interface between the tool and the robot arm adapter.
- **Tool Holder** The component where the tool adapter with its tool is stored.
- **Mount** The connection interface between the tool holder and the Mirte Master
- **V-shape** The shape of the surface that aligns the robot arm adapter to the tool adapter.
- **Tool** The mechanism that is attached to the bottom of the tool adapter.
- **Couple/Attaching** The act of connecting the robot arm adapter to the tool adapter.
- **Decouple** The act of disconnecting the robot arm adapter from the tool adapter.
- **Storing** The act of leaving the tool adapter with the tool disconnected from the robot arm adapter in the tool holder.
- **Tool Operation** The act of using the tools outside of their tool holder, connected to the robot arm adapter.
- **Tool Station** All tool holders and mounts combined. The place where all the tools are stored.
- **Aligning** Ensuring the required positioning of the V-shape of the robot arm adapter and the V-shape of the tool adapter.
- **Pin** The part that securely locks the robotic arm adapter and tool adapter together.
- **Pen** The component responsible for the back-and-forth movement of the pin.

IV. PROJECT GOALS & REQUIREMENTS

Based on the needs of our clients, the project goal and requirements have been set up that define the project's success. This is summarized in the Mission Need Statement:

"To develop a small-scale agricultural tool-switching interface compatible with the Mirte Master, optimized for greenhouse conditions."

Also a goal has been setup that defines when the team is satisfied with the result of the BEP. This is defined in the Project Objective Statement:

"To demonstrate a small-scale, low-budget (max 150 euro) agricultural tool-switching interface compatible with the Mirte Master and at least one of the tools of the parallel group, in normal conditions on both the day of the defense 21th July as the symposium 26th July."

Different levels of requirements can be defined flowing down from these goals. These levels are defined in Appendix B. As these levels all rely on each other, requirements are linked to each other with a parent/child relationship. Starting with Stakeholder requirements that were discovered during meetings with the supervisors and multiple visits to greenhouses of which research surveys are documented in Appendix H. The stakeholder requirements are presented in Appendix M-44. To summarize the system shall be affordable, compatible with the Mirte Master, reliable, as fast as human beings, designed for greenhouse conditions, scalable, easily maintainable and easily manufacturable.

A. System-Level Requirements

First the functional requirements will. These describe what functions or actions the system needs to be able to perform. These are shown in Appendix M-45. To summarize, if the system is capable of coupling, decoupling, holding, storing and operating five tools our mission need statement is achieved.

Each of the functional requirements can be specified by formulating design requirements. They define what shall be designed in order to fulfill all functional requirements. They are shown in Appendix M-46. To summarize for coupling and decoupling of the tools, a mechanical connection between the tools and the robot arm adapter shall be established. For operation of the tools, an electrical connection shall be established. To store the tools they should all fit on the Mirte Master without obstructing its sensors.

Ultimately, the goal is to improve the design of the previous team. This improvement needs to be quantified and can be done by formulating performance requirements. These define how well the functional requirements must be executed. They can ultimately be verified and validated through performance tests which determine the degree of success of the new design. They are presented in Appendix M-47. To summarize, to obtain sufficient reliability, the mechanical and electronical connection should be established at least 1000 times. For this our system needs to be adapted to the accuracy and precision of the Mirte Master's arm which will determine the dimension of our design parameters such as the width and depth of the V-shape. Furthermore to make optimal use of the capabilities of the Mirte Master's arm, we need to optimize the weight as a design parameter such that we can attach tools ranging from 0kg (only tool adapter) to 300grams (maximum tool weight).

These are all the requirements that lead to a successful completion of the system and ultimately the Bachelor End Project.

B. Verification of Requirements

After the complete system has been designed, a verification of requirements must be performed as a proof to our clients that the system works and is improved. Each requirement is assigned one of the four verification methods: Test, Analysis, Demonstration or Inspection defined in Appendix M.

V. FINAL DESIGN

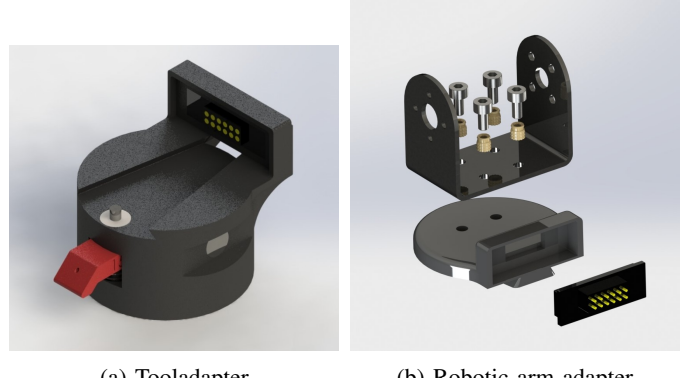
To understand what needs to be improved, the previous design has been thoroughly analysed. This has been done by treating their design as our final product and by performing a verification of the new requirements to the old system. This mock verification is provided in the fifth column of Appendix M. The clarification for this verification is provided through a thorough analysis provided in Appendix C.

In conclusion, the following issues in the current design of the robot arm adapter and tool adapter essential for reliable greenhouse operations have been discovered. The connection mechanism quickly wears out, risking system failure. Electronic connections are exposed to moisture, leading to potential short circuits and reduced lifespan. Dirt accumulation also jams the V-shaped connectors risking more unsuccessful connections. Furthermore, the toolholder does not securely grip tools under dynamic conditions caused by movements of the Mirte Master. Although 3D printing with PLA is convenient as two 3D-printers are at hand, exploring cheaper materials could reduce costs and improve greenhouse resistance. Also the current design's weight exceeds the end-effector's load capacity, forcing tools to be lighter and limiting the Mirte Master's full potential. Critical components like the locking pin have failed during testing, indicating a need for a more robust design of the locking mechanism. Compatibility issues with the Mirte Master require significant downscaling. Lastly, tool switching takes around 20 seconds, which is inefficient and needs improvement.

Now that there is a clear view on the existing problems with the previous design, solutions for any of the unfulfilled requirements presented in Appendix M can be devised. The justification of all of the solutions and decisions result in the final design and is provided in this section. The completely integrated final design is shown in Appendix 19. All designed sub-components are provided in this section in figure 1a (Tool Adapter), figure 1b (Robotic Arm Adapter), figure 2 (Tool Holder), figure 4 (Tool Mount). An overview of all other components is given in Appendix D and the verification of the design is presented in Appendix M. Please also see the system definition in Section III. All technical drawings necessary for manufacturing are provided in L.

A. Wearing of friction surfaces

One of the main stakeholder requirements is that the system shall be as reliable as a human being. This requirement was



(a) Tooladapter

(b) Robotic arm adapter

Fig. 1: Renders tool adapter and robotic tool adapter

not met by the previous design as the locking-pin (figure 25) broke during testing. Preventing this pin from breaking, it is required to reduce the friction/shear force on the pin. First, the pin had to slide across the entirety of the V-shape to be locked because it was extended. To reduce friction caused by the pin, the system was designed such that the pin is retracted in its resting position. This way, the pin is only exposed to normal forces and no shear forces during locking. Furthermore the bolts on the V-shape (figure 15) have been removed and have been replaced by heated inserts (figure 21). This way the wearing of the friction surfaces of the tool adapter and the robotic arm adapter is minimised increasing the lifespan of the system significantly compared to the previous system. These decisions help the design meet requirements SPR-01, SPR-02, SDR-01, SDR-02, SR-06, FSR-01, FSR-02.

B. Moisture Resistance

From our client research (Appendix H) moisture levels were found that are high enough for connections to corrode and electronics to be short circuited. To improve on the previous design, it has been opted to embed the pogo-pin connectors (figure 1a) into the 3d prints, covering the connection surface when connected to the robotic arm adapter. This minimises the chance of moisture getting trapped in small spaces and ultimately the electronic connection. The pogo-pins of this design are water resistant improving the moisture resistance of the electronics significantly compared to the previous design making it more suitable to operate in greenhouse conditions as required. In the previous design leak paths between bolts were present, but have been limited by embedding the connections in the print with heated inserts. This way, it is less likely that moisture gets trapped between bolts which could induce oxidation on the connection points decreasing its lifespan and reliability. The downside of the design is that the magnets used in the tool holder and the tool adapter are exposed and still have leak paths surrounding their diameter which makes them prone to corrosion. When magnets are corroded their magnetic attractive force is weakened [3]. Which could reduce the gripping capability of the tool holder. Embedding the magnets in the 3D-print was an option, but limited the

manufacturability of the design as the 3D-printer had to be paused during the print to place the magnets. These decisions help the design meet requirements SR-07, SR-06, FSR-05, SDR-02, SPR-02, SPR-04.

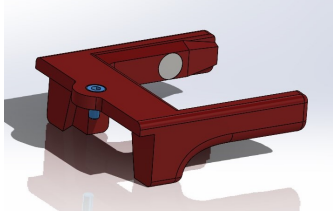


Fig. 2: Tool holder

C. Dirt Resistance

As part of being able to operate in greenhouses, dirt resistance is required as our client research concluded (Appendix H). For this reason the final design has a configuration to cover the upper part of the tool adapter's V-shape by a lid as seen in figure 3. This lid is lifted by the Mirte Master's robotic arm when it is coupling or decoupling the tool adapter. The lid remains closed while the tool is being used, as it will fall back down due to gravity. This way, the tool adapters that are not being used are covered and protected from dirt and organic compounds. In case the dirt still reaches to top of the tool adapter, a hole has been designed in the front of the V-shape seen in figure 1a such that the dirt can be pushed out by the robotic arm adapter when trying to couple. These decisions help the design meet requirements SPR-01, SPR-02, SR-06, SR-07, SDR-01.

D. Tool Gripping Capability of Tool holder

To ensure the tools don't fall out of their tool holder, magnets, strong enough to hold 300 grams vertically, have been added to both the tool holder and the tool adapter. These can be seen in figure 22 and the holes for these magnets are shown in figure 20 and figure 26. The use of magnets minimises the need for a mechanism that locks the tool into the tool holder. The friction of the pen also holds the tool in its place as a second locking mechanism. This ensures that the tool stays firmly in place. The tool adapter has a gripping force of 3.5 newton as calculated in appendix J which is more than enough to hold the maximum tool weight of 300 grams under dynamic conditions. This is a significant improvement to the previous design. These decisions help the design meet requirements SR-02, SR-06, FSR-04, SPR-05, SPR-06, SPR-07.

E. Cost

A bill of materials is provided in Appendix E. As can be seen, the cost requirement SR-01 has been met as we have cut the costs down to 50 euros, which is one third of the total budget. There are still possibilities to cut the costs even more by buying all connections and magnets in bulk.

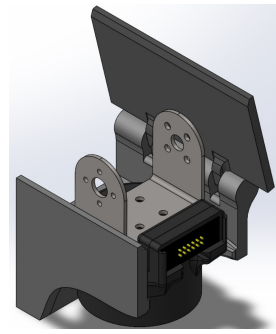


Fig. 3: Lid Anti-Dirt Cover

F. Mass Optimization

The previous design has been scaled down significantly to reduce the mass of the whole system. The diameter of the tool adapter has decreased in size by 25% and the height by 20%. These changes result in a total mass reduction for the tool adapter of 35% from 40 grams to 26 grams. The robotic arm adapter has also been significantly reduced in size such that we obtain a mass reduction of 59% from 34 grams to 14 grams. Making the total design of both the tool adapter and the robotic arm adapter combined weight 40 grams. Compared to the previous mass of 74 grams this is a mass reduction of 46%. This way, tools can be 46% heavier which could lead to more capabilities of the robot. These decisions help the design meet requirements SPR-07.

G. Structural Integrity

To maximize the possible weight of the tools, it was important to reduce the weight of all parts significantly. This comes at the cost of structural integrity if not done properly. With the results of the accuracy & precision tests in VI-A and VI-B, we optimized the design parameters of the V-shape, other dimensions of the tool holder and robotic arm adapter such that they are compatible with the dimensions and precision limitations of the Mirte Master. At the same time, these components should still be able to hold tools of 300 grams and withstand their induced forces. A finite element analysis has been performed to validate the loads on the robotic arm adapter and tool holder in Appendix I. Knowing the limitations of FEM analysis on 3D-printed parts due to its an-isotropic characteristics, we can still deduce that the stress concentrations are well below the yield strength, ensuring the connection to be rigid enough to hold 300 grams on the V-shape. Furthermore the pen (figure 28) has been redesigned as the previous pen broke during testing. Previously the pen and pin were one part, meaning that all the loads had to be transferred through PLA which turned out to be too much. This is why the pen and pin now are made of two different materials and separated from each other as seen in figure 25. It is locked with a split-pin (25) that transfers the loads from the pen to the pin. Finally fillets have been added at locations where the previous design showed high stress concentrations.

These decisions add to the reliability of the system and help meeting requirement SR-06.

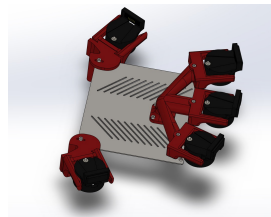


Fig. 4: Configuration of different tool holders

H. Compatibility with Mirte Master

It is required that the tool switch system is compatible with the Mirte Master by requirement SR-02. Therefore the design of the original model has been scaled down significantly. The tool holders which store the tools on the robot are placed on the sides and the back of the robot. Ensuring the impact on the robot's operating space to be minimized. For the attachment of our system to the Mirte Master, all existing holes were reused. Finally the outer dimensions of the entire system has been constrained such that it fits in the original storage box that came with the Mirte Master. These decisions show that compatibility has been considered in all aspects of the design.

I. Scalability

The same system can be used on larger robotic arms under the same conditions. The V-shape can also be easily scaled in size such that it can hold heavier tools. The tool mounts are easily scalable as the number of tool mounts can be altered as a parameter in SolidWorks as can be seen in figure 4. These decisions help the design meet requirement SR-08.

J. Speed

Being faster than a human being is a requirement by our stakeholders that would make the Mirte Master system attractive to buy for companies. After consultation with our supervisors, a tool switch cycle time of 10 seconds would be preferred. The previous system did this in 20 seconds. The cycle time needed to be reduced by half. From our previous design analysis we found that the most time was lost from disconnecting the tools. Their system had to perform a separate action that pushed down the pin to unlock the mechanism. This was our starting point for redesigning the docking/undocking process. The new docking process is depicted in figure 5. Now the docking and undocking can be done using only one and the same movement of the Mirte Master's arm. With a self locking mechanism, the tool adapter first starts in the undocked position with the pen and pin extended by a spring. Ensuring that the robotic arm adapter and the tool adapter stay mechanically connected during operation of the tools. When docking, the pen gets pushed along a slope (figure 5b), such that the pin gets retracted. Then the magnets take over the gripping force of the V-shape, ensuring that the tool adapter stays in the tool holder with the pin retracted. This way all the

tool adapters are ready again to be docked. All of this with just one linear motion of the arm, saving seconds. We have run ten speed tests and came to an average tool switching cycle time of 9.8 seconds. Enough to meet the speed requirement SR-04.

K. Material Choice

The tool switching mechanism will be operating in greenhouses in which the conditions are challenging. A material needs to be selected that can withstand these conditions mentioned before. For the design of the prototypes, PLA was selected due to its ease of manufacturability and availability at the TU-Delft. For actual use in greenhouses, ASA is recommended as it has a high stiffness and resistance against UV, chemicals and increased temperatures. The full derivation of the material selection can be found in appendix O-E.

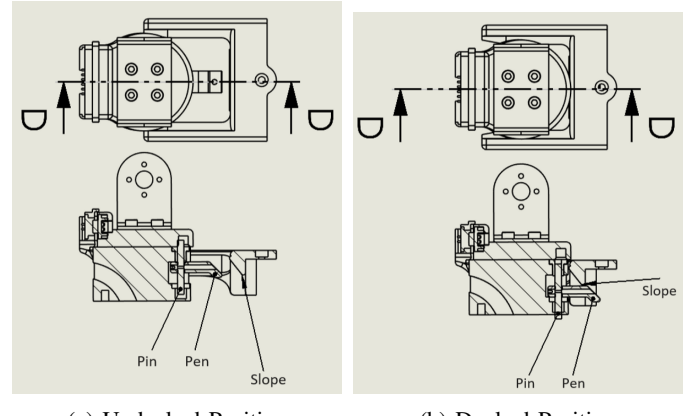


Fig. 5: Configurations of Docking

VI. TESTING

In order to perform a compliance check of the system with the performance requirements, three tests have been setup. These tests have their own research question of which their answer either results in a possible reiteration of our design, or a verified requirement. The first two tests will measure the precision and accuracy of the robotic arm of the Mirte Master. This information will be used to determine the dimensions of the V-shape and the tool holder docking tolerances. Finally the repeatability of the system will be tested which will directly lead back to the reliability and ultimately to all functional requirements.

A. Precision

By determining the influence of our system on the precision of the Mirte Master, mass optimizations can be made, such that all dimensions are just within limits of the Mirte Master's capabilities. Precision is the measure of how consistent the results are when measurements or predictions are repeated under the same conditions. The system needs to couple and decouple the designed adapters shown in figure 7. In order for the V-shape to align the adapter with the connector, the

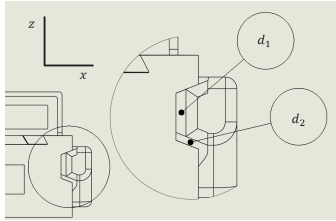


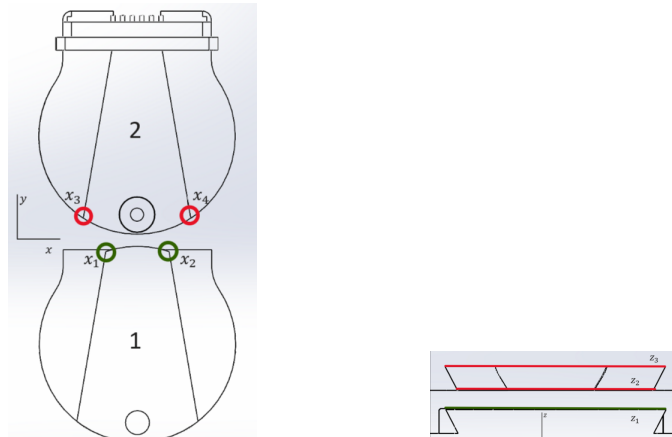
Fig. 6: Docking Precision

design parameters $x_1 > x_3$ and $x_2 < x_4$ have to hold. For the same reason $z_2 < z_1 < z_3$ has to hold and is dependent on the precision in the z-direction defined in figure 7. For the docking location, the precision should be smaller than the design parameters d_1 and d_2 as defined in 6. The final dimensions have been adapted to the outcome of this test result and implemented in a reiteration of the design.

1) *Research Question:* How do different masses [grams] and distances from [cm] the rotation point of the robot arm influence the precision [mm] in x- and z-direction on both the tool docking and tool aligning.

2) *Goal of Test:* Determine the average deviation [mm] in the x- and z-direction between a set of dots marked by the end-effector.

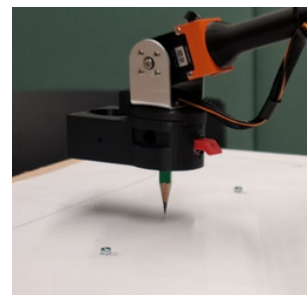
3) *Hypothesis:* It is expected that, as both the mass [kg] increases and the distance where the mass is applied from the rotation point increases, the precision[mm] in both x-direction and z-direction will decrease in random direction. We expect more stochastic vibrations within the servomotors, which will decrease the precision as more mass is added and the applied distance of the mass from the rotation point becomes larger [9]. A scientific substantiation of this hypothesis is provided in Appendix N.



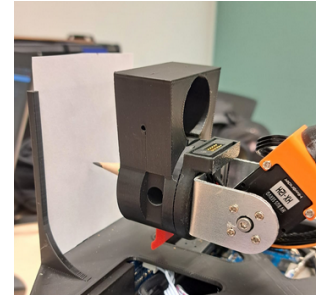
Precision x-direction

Precision z-direction

Fig. 7: V-shape Precision



x-direction setup



z-direction setup

Fig. 8: Accuracy & Precision test setup

4) *Success Criteria:* Since the precision of the system is mainly dependent on the characteristics of the servo motors, our influence on its precision is minimal. A high precision in the movements of the robotic arm is advantageous for the design of the tool switch mechanism and reduces the need for reiterations during the design process. Tweaking the robot's arm movement influences the precision. This can be done by increasing movement time and adding breaks for the system such that vibrations have died out before performing its functions, this will decrease the speed of the system, so a trade-off will have to be made.

5) *Method:* A pencil is rigidly attached vertically to an altered version of the tool holder, with a hole for the pencil and space for masses to be added. This is done to simulate the x and z-direction as shown in figure 7. For measuring the precision in the x-direction a wooden panel has been attached to the top of the Mirte Master covered with a piece of paper. Ten different locations have been marked which represent the pre-docking and docking locations of the robot arm. This setup can be seen in figure 8 and figure 39. For measuring the deflection in the z-direction a 3D printed holder been designed on which a piece of paper could be attached. For both tests different masses ranging from 0 grams (without a tool) to 300 grams (maximum tool weight) are connected to the arm's endeffector. A Python script has been setup which makes the robotic arm place a dot on these ten different positions which can be seen in Appendix K. Figure 39 in the appendix shows these ten different locations on the Mirte Master.

6) *Results:* The test results consist of a set of points in the x-direction and z-direction. There are five measurements for each location (see figure 39) to gain sufficient insight in the spread of the points.

To quantify the results, a standard deviation has been determined (see equation 1) for each of the five measurements per location . These results can be found in Appendix G-31.

$$\sigma = \sqrt{\frac{1}{N} \sum_{i=1}^N (x_i - \mu)^2} \quad (1)$$

The results are further analyzed in figure 9, where the locations are plotted on the x-axis and the standard deviation in mm is plotted on the y-axis. In the chart, each mass is

represented by a specific color, making any trends between the masses clearly visible.

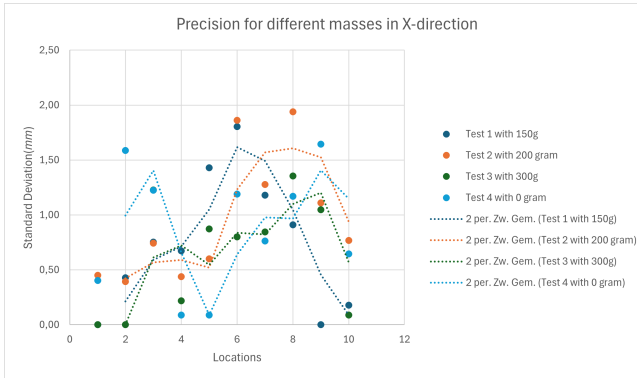


Fig. 9: Standard deviation of the measurements for different masses on 10 different locations in x-direction

Before any conclusions can be drawn from the results, a few remarks regarding the reliability of the results are necessary. The unreliability is caused by several factors. Firstly, half of the locations (5, 6, 7, 8, 9, and 10) of the measurements were programmed, and then these coordinates were mirrored over the other half (1, 2, 3, and 4). The graph clearly shows that the measurements (1,2,3,4) of these locations differ significantly, while in theory they should match with the measurements (7,8,9,10). Therefore, we exclude these measurements from the analysis. In addition, there is an unreliability factor in the arm. During the test, there were moments when the servos in the arm stalled, causing the end to make slight trembling movements. This caused measurement points to deviate exceptionally high or low.

Nevertheless, there are some trends visible in the results. Firstly, clear parabolic trend lines can be seen for all masses from location 5 to 10. These trend lines peak particularly at locations 6 to 8, leading to the conclusion that precision decreases with target points at greater distance from the origin, or a longer arm. Now the distances between the trend lines, or rather the influence of mass on precision, are being considered. However, these results did not clearly emerge from the test. In particular, the standard deviation of test 4 at 0g significantly differs from other trend lines. When this is disregarded, it can be concluded that test 2 at 200 grams has the highest standard deviation and thus the lowest precision. Following that, is the test at 150 grams and lastly the test at 300 grams. A notable result is that precision at these higher masses is significantly less dependent on the length of the arm, or the distance of the target to the origin. This could be explained by the higher moment of inertia of the system at these masses, that increases the damping effect of vibrations which could lead to an improved control response [15].

In the z-direction 5 measurements per different mass were taken. However, these measurements were not taken at different locations due to limited resources. The results of these measurements show a clear trend between the higher masses

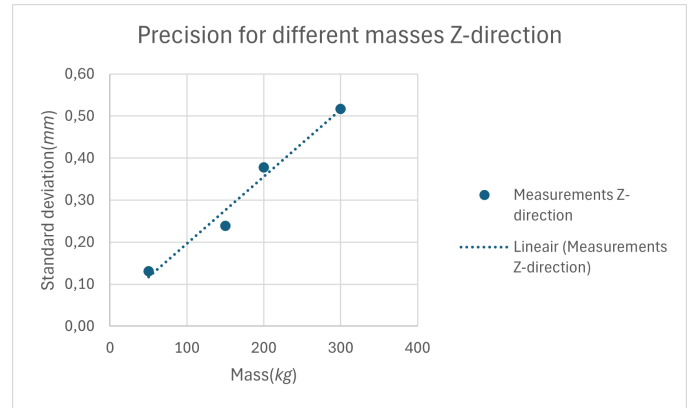


Fig. 10: Calculated deviation for different masses in z-direction

and the standard deviation. From this increasing deviation trend, it can be concluded that the precision decreases in the z-direction with higher mass attached. Which could be explained by the increase in moment and therefore deformation as explained in Appendix N. The effect of these results on our design will be discussed in VII.

B. Accuracy

Besides determining the precision , it is also important to determine it's accuracy to align the robot arm adapter and the tool adapter within the to be designed tolerances. The average deviation of a measured value compared to it's set actual value. As the mass of the tools increases, it might be necessary for the robotic arm to compensate in the z-direction for the deflection caused by this increase in mass. Influences on the programming of the robotic arm can be made to account for this deflection which causes this decrease in accuracy. Increased mass mostly impacts accuracy in the z-direction, therefore only accuracy in the z-direction was tested.

1) *Research Question:* How do different masses [kg] and distances from the rotation point of the robot arm [cm] influence the accuracy [mm] in z-direction?

2) *Goal of Test:* Determine the deflection of the robotic arm so adjustments can be made to the movement of the robotic arm to increase the overall reliability of the system.

3) *Hypothesis:* It is expected that, as the mass [kg] increases and the distance [cm] from the rotation point increases, the accuracy [mm] in z-direction decreases linearly as a cause of the increase in mass [kg] and to the power of 3 as a cause of the increase in distance [mm]. For the torsion in the gears of the servo we expect the accuracy to decrease linearly both for the increase in mass [kg] and increase in distance [cm]. The influence of the deformation of the arms is expected to be negligible, whereas the influence of the internal deformation of the servomotors is considered to be significant. A thorough scientific substantiation of the hypothesis is provided in Appendix N-A.

4) *Success Criteria:* As mentioned in the previous test, the robotic arm has been provided, so our influence on it's

performance is minimal. A small deflection in the z-direction of the robotic arm is advantageous as it minimises the need for compensation in the z-direction.

5) *Method:* The accuracy test is conducted in the same manner as the precision test, see figure 8. The same raw data is used here as well as in figure 32, but it is analyzed differently.

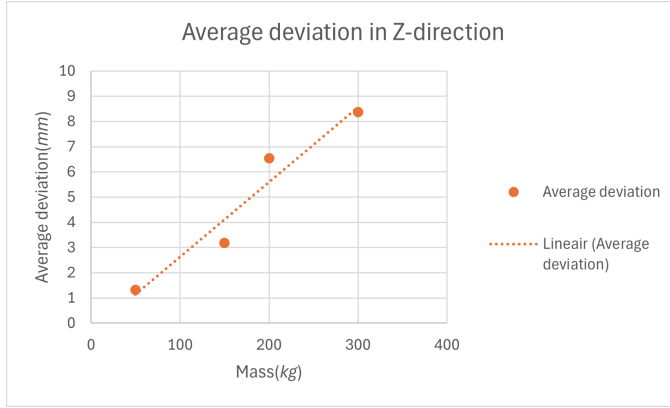


Fig. 11: Results accuracy z-direction

6) *Results:* As previously mentioned, the accuracy test is only measured in the z-direction. For the accuracy test, it is particularly important to understand the effect of the mass on the accuracy. Therefore, an average of the five measurements is taken per mass. This makes it easier to process the results in a clear manner. The results are shown in a graph with the different masses on the x-axis and the average deviation per mass on the y-axis.

There is a clear trend in the accuracy decrease at a higher mass. So as predicted in the hypothesis, deviation is greater with higher masses. This consequently results in lower accuracy. The effect of these results on our design will be discussed in VII.

C. Repeatability

The tool switching mechanism will be used in greenhouses for a longer period of time. Therefore this system needs to withstand many duty cycles. A high repeatability makes the system reliable and contributes to the overall efficiency of the robot.

1) *Research Question:* How does the attached mass [grams] influence the reliability (%) of mechanically and electronically coupling and decoupling of the toolswitch mechanism?

2) *Goal of Test:* To answer this research question, a test has been carried out which determines the repeatability ratio between successful and unsuccessful dockings (mechanically and electronically).

3) *Hypothesis:* It is expected that the reliability [%] of the system will decrease as the mass [kg] increases. A scientific substantiation is provided in Appendix N-C.

TABLE I: Repeatability of different runs

Run	Runs	Mass [g]	Sides	Back	Total %	Remarks
1	99	300	100%	100%	100%	Untuned
2	99	100	93.9%	100%	96.0%	Untuned
3	99	300	97.0%	100%	97.9%	Untuned
4	198	100	99.1%	100%	99.5%	Tuned
5	198	300	98.5%	97.0%	98.0%	Tuned

4) *Success Criteria:* The reliability of a human is 100% as a human being will always be able to switch tools. So a reliability of almost a 100% needs to be achieved, which is unrealistic. The goal has been set to significantly improve reliability compared to the previous group which was 83.1 %. Therefore a success rate above 90% is considered to be successful.

5) *Method:* A Python script has been setup (Appendix K) to switch between three different tool holders on the Mirte Master as depicted in figure 12. Per location the robot coupled and decoupled the tool 33 times which returned a total of 99 data points per run. A maximum mass of 300 grams was used and a minimum mass of 100 grams. In total 693 data points were collected. The previous group had 50 data points in total for repeatability. If both the minimum and maximum mass attain a reliability over 90%, the test is considered successful. The coupling of the robotic arm with the tool is considered successful if an electrical connection has been made between the tool-adapter and the robotic arm adapter. The electrical connection between is measured using the schematic in figure 40. In order to control the environment, the Mirte Master has been connected to a variable power supply which gives a constant voltage to cancel out any effects caused by the battery percentage.

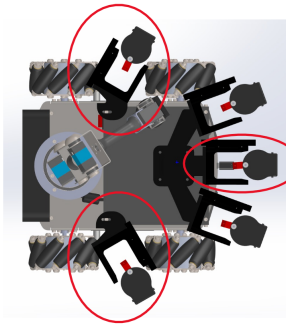


Fig. 12: Test Setup Repeatability

6) *Results:* From the data in table I can be concluded that the system has achieved the desired result. A repeatability of at least 90% has been achieved every single run. It was expected that an increased mass would negatively impact the repeatability of the system. Results of the first three runs contradicted this hypothesis, as tools with a greater mass achieved a higher repeatability score. This obtained result could be explained by the behaviour of the robotic arm. While trying to connect to the tools on the sides of the robot, the robotic arm gave these tools a slight push. This resulted in the

tool shifting slightly out of the toolbox. Consequently, when the arm tried to connect to the tool, it was pushed out of the tool holder. The lighter tools were affected more by this push. Tuning the arm improved docking the tools on the side of the robot as can be seen from the results from the fourth and fifth run. The repeatability of the lighter tool now exceeds that of the heavier tool and this aligns with the hypothesis. The effect of these results on our design will be discussed in VII.

VII. DISCUSSION AND RECOMMENDATIONS

To assess the performance of the Mirte Master and our system, three tests have been carried out. The results are insightful and provide clear parameters for design adjustments.

First, the precision test was conducted, where the standard deviation was calculated and compared with different masses. This data was used to optimize the tool adapter and robot arm adapter using the parameters described in figure 7. The maximum deviation is determined by taking 3σ . With this deviation, 99.73% of the measurements fall within this range (see figure 54).

For the x-direction, the maximum deviation ($\sigma = 1.94$ mm) was measured in Test 2-200 grams at location 8. This results in $3\sigma = 5.82$ mm. Consequently, the design must be adjusted to meet the following equation: $(x_4 - x_3) - (x_2 - x_1) = 5.82\text{mm}$ (see figure 7).

This calculation is also done in the same way for the Z-direction. For this, the maximum deviation found is $\sigma = 0.52$ mm, leading to $3\sigma = 1.56\text{mm}$. With this given, the tool-switching system must therefore meet the equation $z_3 - z_1 = 1.56\text{mm}$ (see figure 7) to operate successfully in > 99% of cases. This results from the accuracy test provides insight into the deflection of the robotic arm. The test is only conducted at one position of the robotic arm. To get a better insight in the overall deflection of the arm it would be beneficial to conduct the test at different locations further and closer away from the base of the arm. This is valuable information and can provide a better insight into the corrections that need to be programmed for the robotic arm to dock tools at different locations. The results from the repeatability tests show that the tool switch mechanism is able to operate successful for a longer period of time. The system has been tested for 693. For future research it would be valuable to verify repeatability for an even longer period of time. Also the it has not been tested how the repeatability is affected by greenhouse conditions.

While design decisions have been made to make sure that the system is water resistance, this has not been thoroughly tested and verified. This is mainly because the Mirte Master is not yet capable of withstanding high humidity ranges.

Chemical resistance during operation in the greenhouses have not been quantified as the priorities of our supervisors changed during the project. Since chemicals are used in greenhouses, a study on this and the impact on the durability of the system would be insightful.

While the most UV resistant 3D-print has been chosen (ASA). UV intensities have not been quantified by the team leading to an untested performance requirement SPR-08. Since the

system has not been tested under these challenging conditions, its capabilities in greenhouses remain unverified. Testing the system in these rough conditions would provide relevant data about the system's operation.

Parallel to the development of this system, another BEP group has developed several tools. It would be interesting to integrate these projects and assess whether the system works well and see if adjustments have to be made.

VIII. CONCLUSION

The mission for this project was to develop a small-scale agricultural tool-switching interface compatible with the Mirte Master optimized for greenhouse conditions. A NASA systems engineering & project management approach had been used to meet the mission need statement [7]. After performing all of the project phases, the result is a fully functional tool switching system with capabilities of operating in a greenhouse.

The design solutions have been verified against the requirements by performing the compliance methods: analysis (Appendix I), tests (Section VI), inspections (Section V) and demonstrations during supervisor meetings. The performance of the system has been evaluated by several tests among which the repeatability tests. The system got a repeatability of 99.5% for tools with a mass of 100 grams and 97.8% for tools with a mass of 300 grams. This is a significant improvement compared to last year's system which achieved a repeatability of 83.1%. The new tool switch interface is significantly smaller and its mass has been reduced by 46%. This opens doors for future research groups to study the functionality of the Mirte Master in greenhouses.

With all functional, design and most of the performance requirements met, the final design can be considered as a full-scale working toolswitching system, optimized for the Mirte Master. With further research on the integration of the Mirte Master in greenhouses, Mirte Master can make a difference for owners of smaller greenhouses using the designed tool switch mechanism.

ACKNOWLEDGEMENTS

Supervisors:

Dr. C. Pek

Prof.Dr.Ir. M. Wisse

Dr. Ir. G.N. Saunders

Technical support:

Ir. A. van Hilten

REFERENCES

- [1] Admin. *Eliminating backlash*. May 2024. URL: <https://imsystems.nl/backlash/>.
- [2] Webcraft Ag. *Verschil tussen houdkracht en (af)schuifkracht*. URL: <https://www.supermagnete.nl/faq/Waarin-verschillen-de-houdkracht-en-de-verschuifkracht-afschuifkracht-van-elkaar>.
- [3] Khalid A. Ahmad et al. “Magnetic strength and corrosion of rare earth magnets”. In: *American journal of orthodontics and dentofacial orthopedics* 130.3 (Sept. 2006), 275.e11–275.e15. DOI: 10.1016/j.ajodo.2006.01.024. URL: https://www.sciencedirect.com/science/article/abs/pii/S0889540606007086?casa_token=YWRh1tyq4BUAAAAA:5GIcOQnzfkGdAqOp1zQbXfq1KwbeFyscRoSgKOyrMnJJgCmH3JODgFVHit48hnAqY-SFZVzCVE.
- [4] Joseph S. Weaver Ph. D. *Normal distribution*. July 2018. URL: <https://mypages.svsu.edu/~jweaver/8/NormalDistirbution.html>.
- [5] Charles De Kergariou et al. “The influence of the humidity on the mechanical properties of 3D printed continuous flax fibre reinforced poly(lactic acid) composites”. In: *Composites. Part A, Applied science and manufacturing* 155 (Apr. 2022), p. 106805. DOI: 10.1016/j.compositesa.2022.106805. URL: <https://doi.org/10.1016/j.compositesa.2022.106805>.
- [6] Gear Technology India and Gear Technology India. *Understanding Backlash in Bevel Gears: Causes, Effects, and Solutions - Gear Technology India*. Sept. 2023. URL: <https://www.geartechnologyindia.com/understanding-backlash-in-bevel-gears-causes-effects-and-solutions/>.
- [7] NASA. *Systems Engineering Handbook*. National Aeronautics and Space Administration NASA Headquarters Washington, D.C. 20546, 2007.
- [8] Wojciech Pawlak. “Wear and coefficient of friction of pla-graphite composite in 3D printing technology”. In: *Engineering Mechanics* ... (May 2018). DOI: 10.21495/91-8-649. URL: https://www.researchgate.net/publication/330003074_Wear_and_coefficient_of_friction_of_PLA_Graphite_composite_in_3D_printing_technology.
- [9] Massimiliano Rigacci, Ryuta Sato, and Keiichi Shirase. “Evaluating the influence of mechanical system vibration characteristics on servo motor efficiency”. In: *Precision Engineering* 72 (Nov. 2021), pp. 680–689. DOI: 10.1016/j.precisioneng.2021.07.012.
- [10] Sanne Schelfaut. *DPG Media Privacy Gate*. Jan. 2020. URL: <https://www.ad.nl/koken-en-eten/nederland-is-de-op-een-na-grootste-landbouwexporteur-ter-wereld~a555352f/?referrer=https%3A%2F%2Fwww.google.com%2F>.
- [11] Jesse Schevel. *Europees ‘Tinder voor banen’-plan moet tekorten arbeidsmarkt uit derde landen invullen*. Nov. 2023. URL: <https://www.glastuinbouwnederland.nl/nieuws/europees-tinder-voor-banen-plan-moet-tekorten-arbeidsmarkt-uit-derde-landen-invullen>.
- [12] Simplify3D Software. *Ultimate 3D Printing Material Properties Table*. Nov. 2022. URL: <https://www.simplify3d.com/resources/materials-guide/properties-table/>.
- [13] *Understanding area expansion*. Mar. 2022. URL: <https://unacademy.com/content/cbse-class-11/study-material/physics/area-expansion/>.
- [14] Anton Van Beek. *Advanced engineering design : lifetime performance and reliability*. Jan. 2009. URL: <https://lib.ugent.be/en/catalog/rug01:001987805>.
- [15] Fang Xie, Fei Yu, and Chaochen An. “Research on Dynamic Identification of Servo Motor Load Inertia Based on the Error Gain Factor Model”. In: *Energies* 14.20 (2021). ISSN: 1996-1073. DOI: 10.3390/en14206664. URL: <https://www.mdpi.com/1996-1073/14/20/6664>.
- [16] *Yizhet 50 stuks magneeten huishoudelijke magneeten 8x3 mm mini magneet voor magneetbord, whiteboard, bord, prikbord, koelkast enz. (8 x 3 mm)*.

APPENDIX A
PROJECT MANAGEMENT PLAN

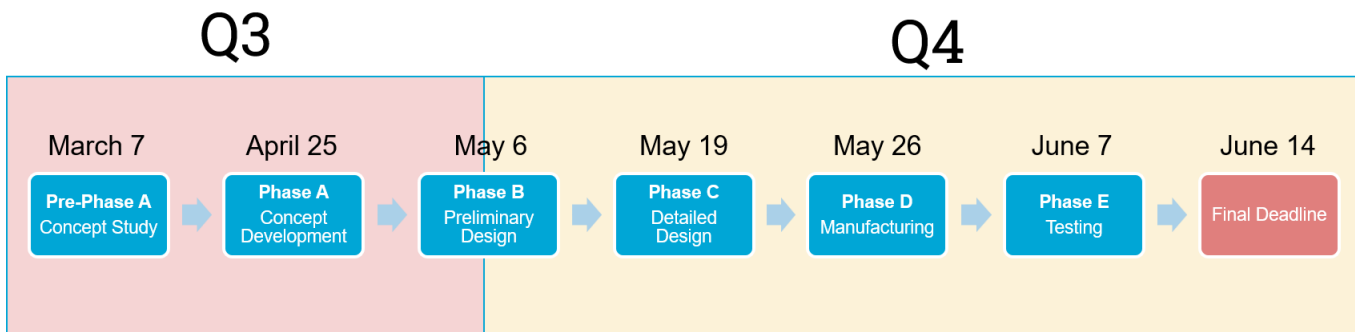


Fig. 13: Project Planning

APPENDIX B
REQUIREMENT LEVELS

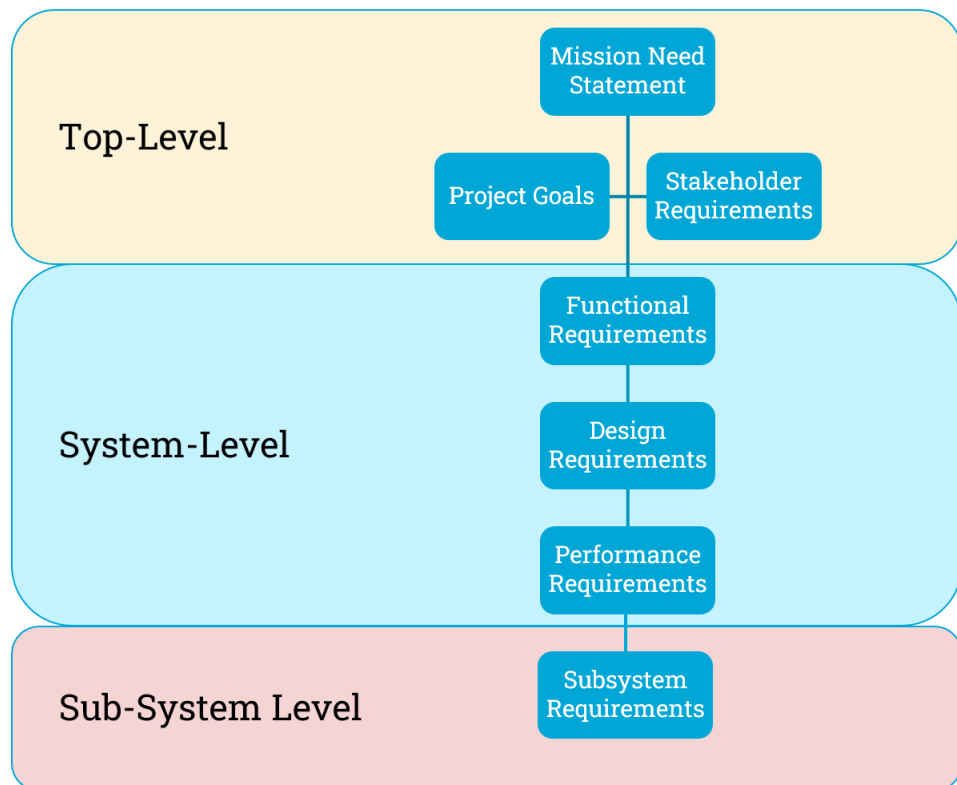


Fig. 14: Levels of Requirements

APPENDIX C

PREVIOUS DESIGN ANALYSIS

This section is an overview of all the issues found with relation to which requirement and describes our initial ideas on how to improve them in our design. The definitions of all systems are provided in III

A. Wearing of friction surfaces

A test has been performed in which the robot arm adapter has connected and disconnected the pin 100 times. It was concluded that the connection mechanism in figure 15 was wearing out the surface underneath in such a rate that it could not connect anymore at some point. This would result in the failure of our system.

- 1) Failed Requirements: SPR-01, SPR-02, SDR-01, SDR-02, SR-06, FSR-01, FSR-02.



Fig. 15: Wearing of Friction Surfaces

B. Moisture Resistance

Per visual inspection, it can be seen that the electronic connection between the robot arm adapter and the tooladapter is exposed to the outside as depicted in figure 16. From our client research observations in the greenhouses (Appendix H) it turned out that the moisture levels are significant (sometimes above 80%). This makes their design prone to circuit shorting and a decreased lifetime. Which makes the system less reliable and safe to use. The aim is to integrate all electrical connections on the inside of our design to protect them against drops of water and dirt.

- 1) Failed Requirements: SR-07, SR-06, FSR-05, SDR-02, SPR-02, SPR-04.

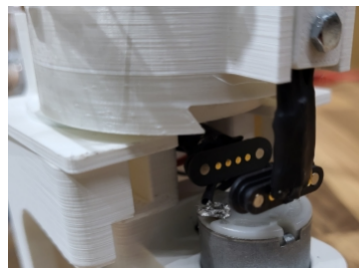


Fig. 16: Exposed Electronics

C. Dirt Resistance

Per visual inspection, it can be seen that the V-shape is exposed. During our client research, it was found out that the environment of the workers in the greenhouses can become quite dirty (Appendix H). To quickly test the effects of this amount of dirt in the form of sand grains on the V-shape, it was found out that the tool couldn't connect properly anymore because the dirt on the V-shape was jamming the robot arm adapter.

- 1) Failed Requirements: SPR-01, SPR-02, SR-06, SR-07, SDR-01.

D. Tool Gripping Capability of Toolholder

A mass of 100 grams was hung on the pin in their toolholder. It almost immediately fell off when shaking the toolholder slightly. Also the tool was not rigidly attached to the toolholder while stationary.



Fig. 17: Exposed V-shape

1) Failed Requirements: SR-02, SR-06, FSR-04, SPR-05, SPR-06, SPR-07. Their system was designed on a static plate, while our system needs to be carried on a moving Mirte Master.

E. Cost

Almost all parts are 3D-printed and made from PLA. It was chosen to 3D-print as much as possible as two teammates in our group (Fedde & Jasper) have a 3D-printer with PLA so this can drive down the cost as well. This already helps meeting requirement SR-01.

F. Mass Optimization

The maximum weight that can be added on the end-effector is 0.3 kg. The tools are in the end the ones that need to perform the more top-level functions of the entire system. To ensure that the tools can be as heavy as possible, this automatically means that our tool switching mechanism needs to be as light as possible. Currently their design of the tool switching system that needs to be attached to the robot arm is around 100 grams. By inspection many possibilities were seen to remove the mass. As can be seen in figure 18, there are bolts sticking out at location 2. These do not have any structural purpose so we will make them fit in our design. In location 1 there is a plate of PLA that serves no structural or functional purpose. As the system functions without it, so we can get rid of it in our design. At location 3 a diameter of 6cm can be seen, with the new Mirte Master, this is too large so can diminish the diameter and save weight of the pin. At location 5, the rails for the tool to fit in the tool holder can be seen. It may be possible to eliminate it by integrating these rails inside the pin. With these changes, 50 grams of weight can be saved such that half of the weight can be cut from the previous design.

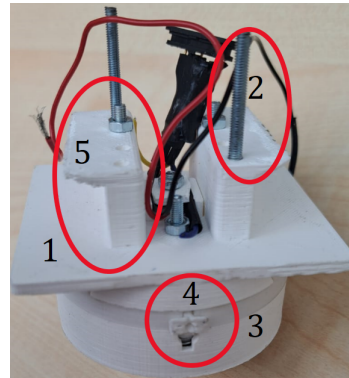


Fig. 18: Mass Efficiency of Previous Design

G. Structural Integrity

As can be seen in figure 18 at location 4, the pin that was responsible for locking the robot arm adapter with the pin broke off during a physical examination by one of our professors. This is a crucial part of the design that cannot fail as it will lead to instant failure of the operation of the tools as they will fall off.

1) Failed Requirements: FSR-03, FSR-05.

H. Compatibility with Mirte Master

The system has not been designed to work with the hardware and software of the Mirte Master. The pin's diameters are too big for the end-effector of the Mirte Master's arm. Also the toolholders are too large if the goal is to put five tool holders like theirs on the Mirte Master. Significant downscaling is necessary to make all the tools fit on the Mirte Master.

1) Failed Requirements: SR-02

I. Scalability

One of our stakeholder requirements is that our supervisors would love to see our system to be scalable. The toolstation is designed to be modular, this means that more tools can be added simply by enlarging the toolstation's geometry. This is a feature intended to be retained in the design. Though because of the lack of mass optimization of their design, the system would become too heavy for the current arm to scale. The SolidWorks models should be designed in such a way, that the main design parameters can be scaled easily without loss in performance.

1) Failed Requirements: SR-08

J. Speed

It is tested how fast a tool can be switched with its arm. This takes around 20 seconds. An attempt can be made to try to diminish the amount of actions needed to decouple and couple the tools.

1) Failed Requirements: SR-04

K. Requirement Verification of Previous Design

As a summary to this analysis, a verification matrix can be filled in, that gives an overview of which requirements are already fulfilled by the previous design and which aren't. The full verification matrix can be found in Appendix M.

APPENDIX D
DESIGN OVERVIEW

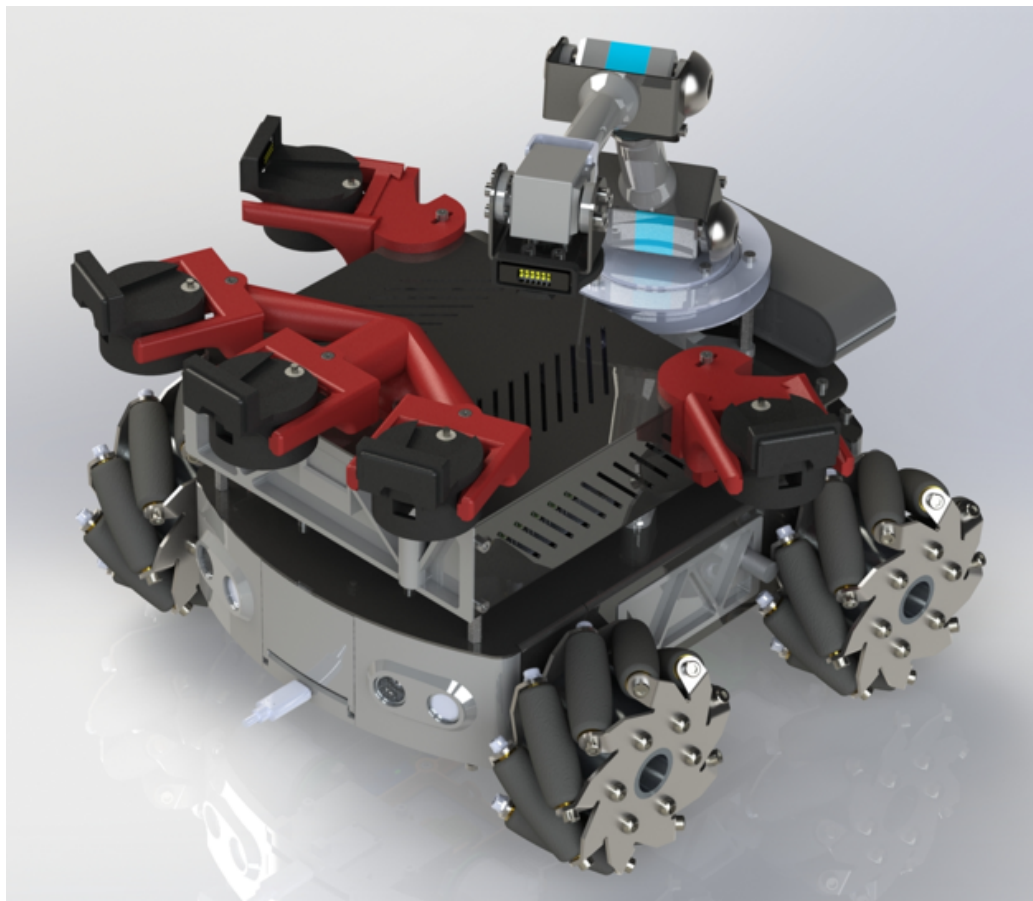


Fig. 19: Total Design Integration

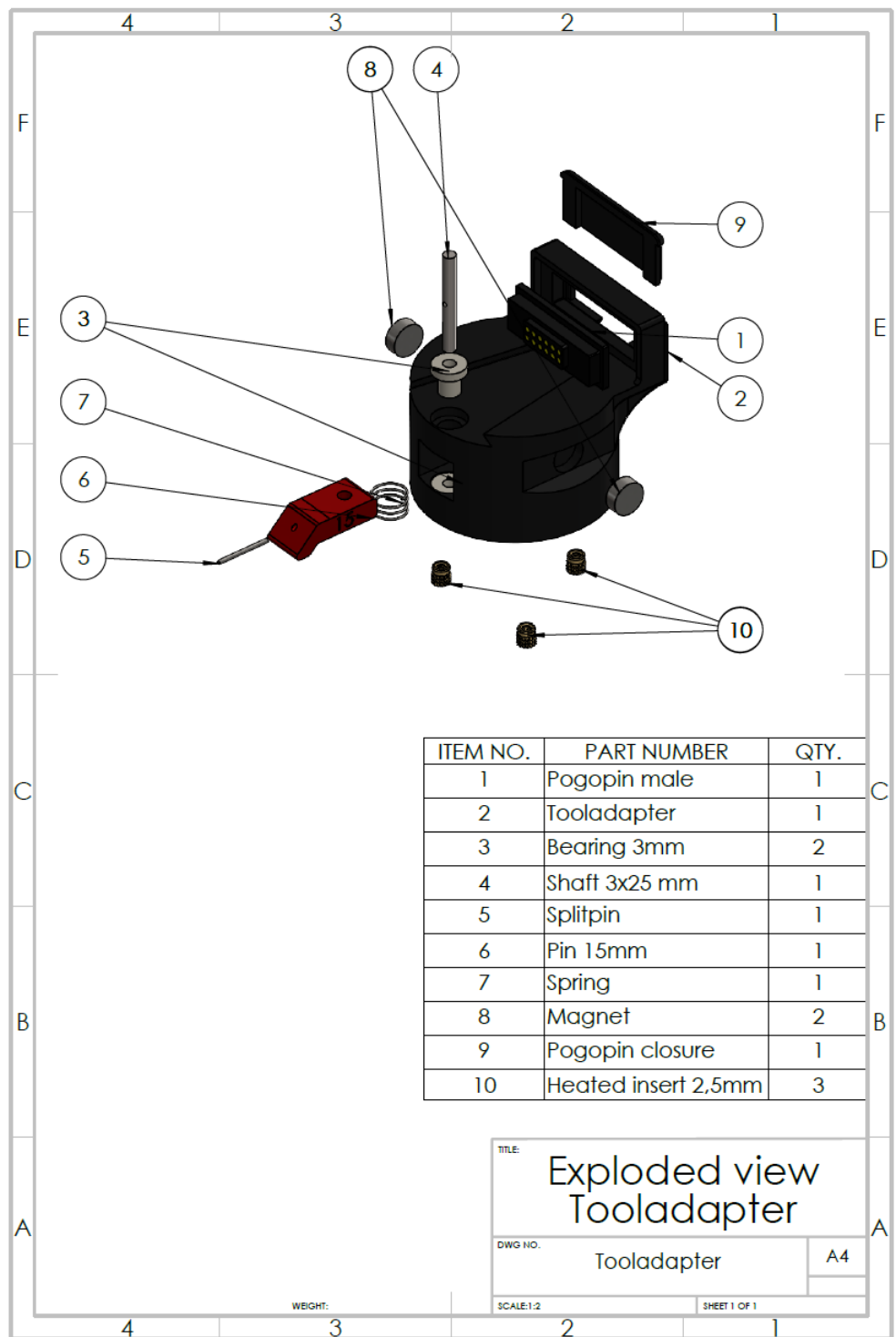


Fig. 20: Tooladapter Overview

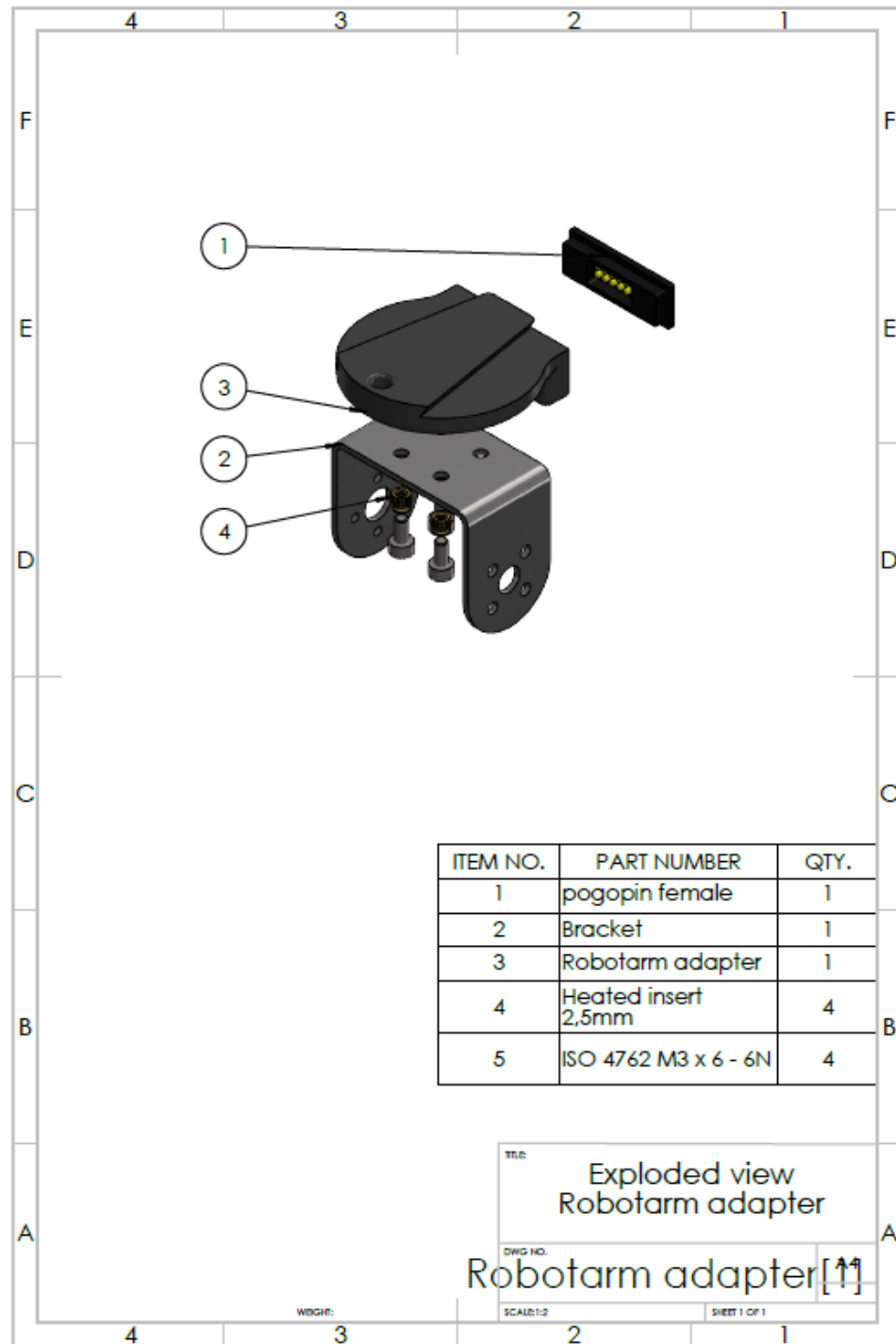


Fig. 21: Robotic Arm Adapter Overview

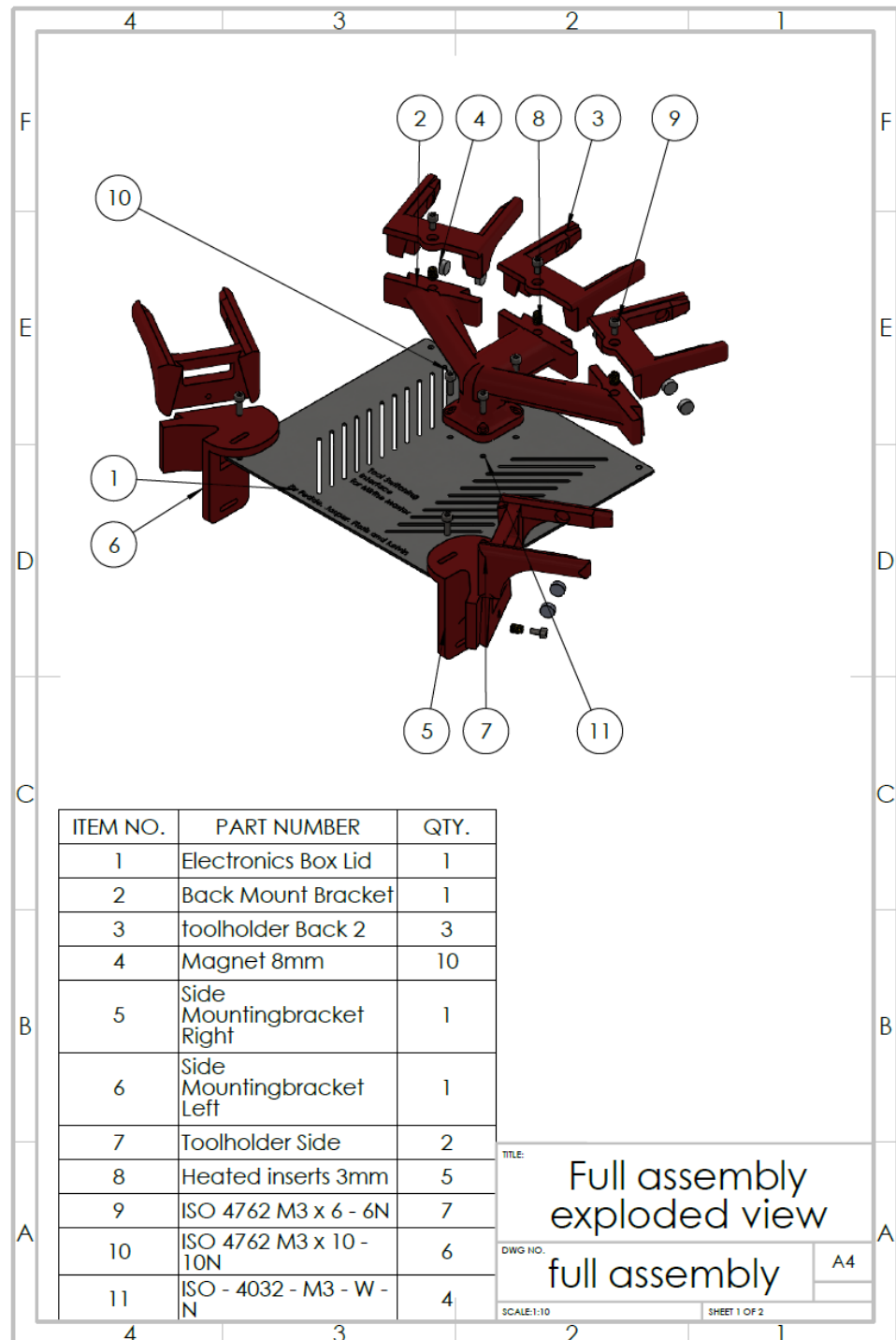


Fig. 22: Toolstation Overview

APPENDIX E
BILL OF MATERIALS

The bill of materials is based on the configuration with 5 tools. Some elements have been bought in bulk, so the price might vary depending on where you buy it and how much you buy. This list is a rough overview and price estimation of our system. This assumes all IWS materials to be free and all the 3D printed parts to be able to printed with 1 roll of PLA. The item numbers in column 1 correspond to Tooladapters in figure 25, Robotic Arm Adapter in figure 21 and Toolstation in figure 22.

Tooladapters							
Item No.	Part Number	Qty.	Cost per piece	Total Cost	Where to get?	URL	How to manufacture?
1	Pogopin Male	5	€1,43	€7,17	Aliexpress	spm=a2g0o.order_detail.orc	Of the shelf
2	Tooladapter Frame	5	X	X	X	X	3D Print
3	Bearing 3mm	10	X	X	IWS	X	Of the shelf
4	Shaft 3x25mm	5	X	X	IWS	X	Saw & Drill
5	Splitpin	5	X	€2,95	HEMA	ce=1&gclid=CjwKCAjwjqWzE	Of the shelf
6	Pin 15mm	5	X	X	X	X	3D Print
7	Spring	5	X	€4,00	Hornbach	ssortimentsdoos-trek-en-dr	Cut to size
8	Magnet	10	€0,18	€ 1.80	Amazon	i074C79DJS?ref=ppx_yo2ov	Of the shelf
9	Pogopin Closure	5	X	X	X	X	3D Print
10	Heated Insert 2.5mm	15	€ 0.35	€5,25	Mouser	439722&gad_source=1&gcl	Of the shelf

Robotic Arm Adapter							
Item No.	Part Number	Qty.	Cost per piece	Total Cost	Where to get?	URL	How to manufacture?
1	Pogopin female	1	€2,66	€2,66	Aliexpress	spm=a2g0o.order_detail.orc	Of the shelf
2	Bracket G	1	X	X	IWS	X	Lasercut
3	Robot Arm Adapter	1	X	X	X	X	3D Print
4	Heated Insert 2.5mm	4	€0,35	€1,40	Mouser	439722&gad_source=1&gcl	Of the shelf
5	Bolts M2.5x6mm	4	X	X	IWS	X	Of the shelf

Toolstation							
Item No.	Part Number	Qty.	Cost per piece	Total Cost	Where to get?	URL	How to manufacture?
1	Electronics Box Lid	1	X	X	IWS	X	Lasercut
2	Back Mount Bracket	1	X	X	X	X	3D Print
3	Tool Holder Back	3	X	X	X	X	3D Print
4	Magnet	10	€0,18	€1,80	Amazon	i074C79DJS?ref=ppx_yo2ov	Of the shelf
5	Side Mounting Bracket Right	1	X	X	X	X	3D Print
6	Side Mounting Bracket Left	1	X	X	X	X	3D Print
7	Toolholder Side	2	X	X	X	X	3D Print
8	Heated Inserts 3mm	5	€0,46	€2,30	RS	ts_-2040621&matchtype=	Of the shelf
9	Bolts M3x6	7	X	X	IWS	X	Of the shelf
10	Bolts M3x10	6	X	X	IWS	X	Of the shelf
11	Bolts M3xW	4	X	X	IWS	X	Of the shelf

Extra							
	PLA	1	€27,50	€27,50	123-3D	ml?gad_source=1&gclid=Cj	Of the shelf
Total				€56,53			

Fig. 23: Bill of Materials

APPENDIX F
3D PRINTED PARTS

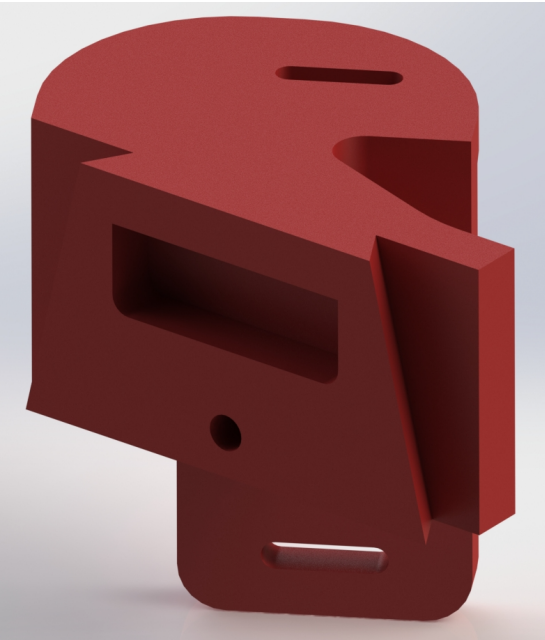


Fig. 24: Toolmount Sides 3D-Print (Item No. 5&6 in figure22)

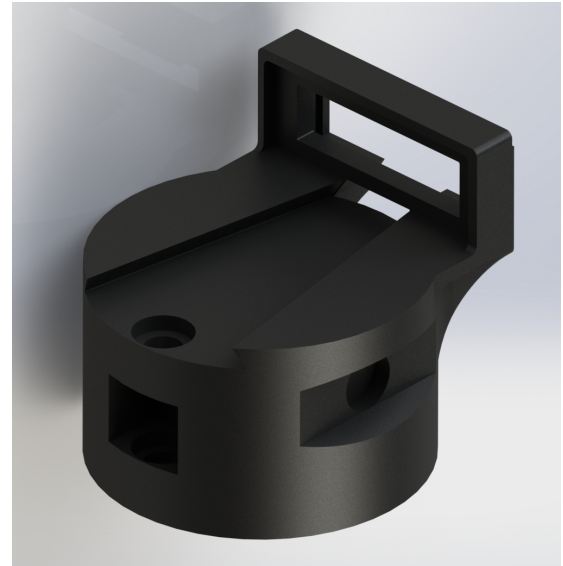


Fig. 25: Tooladapter 3D-Print (Item No. 2 in figure 25)



Fig. 26: Toolholder Back 3D-Print (Item No. 7 in figure 22)



Fig. 27: Toolmount Back 3D-Print (Item No. 2 in figure 22)

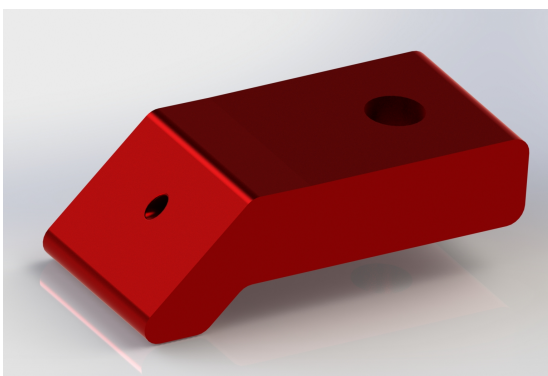


Fig. 28: Pen 3D-Print (Item No. 6 in figure 25)

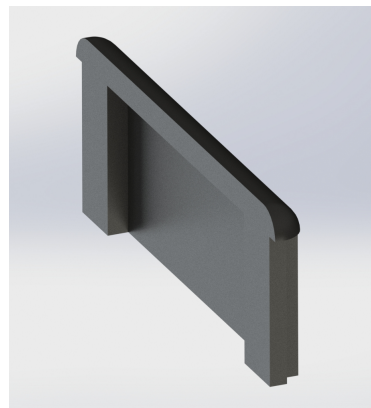


Fig. 29: Pogopin Closure (Item No. 9 in figure 25)

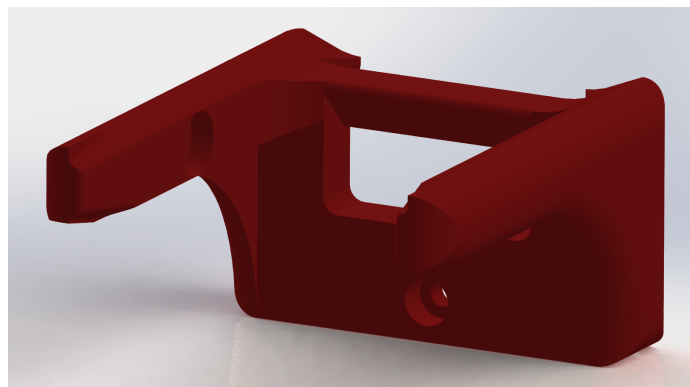


Fig. 30: Toolholder Side 3D-Print (Item No. 7 in figure 22)

APPENDIX G

TEST RESULTS

Test 1 with 150g

Location	Measurements					Standard deviation	Average
1	0,6	0,6	0,6	0,6	0,6	0,00	0,60
2	0,3	0,2	1,2	0,3	0,2	0,43	0,44
3	1,2	2,1	3,0	1,2	2,1	0,75	1,92
4	5,9	6,5	7,0	7,7	6,5	0,67	6,72
5	2,9	3,8	3,8	0,5	3,8	1,43	2,96
6	0,7	3,7	4,6	5,5	3,7	1,80	3,64
7	0,9	1,7	1,7	2,9	3,9	1,18	2,22
8	1,6	2,5	3,2	3,3	4	0,91	2,92
9	1,1	1,1	1,1	1,1	1,1	0,00	1,10
10	2,1	2,5	2,5	2,5	2,5	0,18	2,42

Test 2 with 200 gram

Location	Measurements					Standard deviation	Average
1	2,0	3,1	2,3	2,0	2,3	0,45	2,34
2	1,7	2,6	2,5	2,6	2,6	0,39	2,40
3	2,7	4,3	4,5	4,3	4,3	0,74	4,02
4	1,5	0,5	1,4	1,5	1,5	0,44	1,28
5	2,4	2,4	1,2	1,2	1,7	0,60	1,78
6	1,1	3,9	5,0	6,1	4,2	1,86	4,06
7	1,1	4,3	3,2	1,8	1,9	1,28	2,46
8	1,1	4,2	5,2	6,3	4,3	1,94	4,22
9	3,0	6,1	4,3	4,6	4,8	1,11	4,56
10	1,0	2,4	2,4	1,0	1,0	0,77	1,56

Test 3 with 300g

Locations	Measurements					Standard deviation	Average
1	0,7	0,7	0,7	0,7	0,7	0,00	0,70
2	1,9	1,9	1,9	1,9	1,9	0,00	1,90
3	7,3	9,3	8,7	10,7	9,3	1,23	9,06
4	3,5	3,5	3,9	3,9	3,9	0,22	3,74
5	1,9	2,7	3,9	3,7	3,8	0,87	3,20
6	4,5	5,3	6,3	6,3	6,2	0,80	5,72
7	3,5	2,0	4,1	3,6	4,0	0,84	3,44
8	0,8	2,9	4,6	3,0	3,1	1,36	2,88
9	1,0	1,2	1,2	2,5	3,4	1,05	1,86
10	3,2	3,2	3,2	3,1	3,0	0,09	3,14

Test 4 with 0 gram

locations	Measurements					Standard deviation	Average
1	1,4	0,5	0,5	0,5	0,50	0,40	0,68
2	0,5	0,5	3,0	3,6	3,50	1,59	2,22
3	2,0	2,0	3,0	3,0	5,00	1,22	3,00
4	7,3	7,3	7,2	7,3	7,10	0,09	7,24
5	5,3	5,3	5,2	5,3	5,10	0,09	5,24
6	7,1	8,5	10,1	9,6	9,50	1,19	8,96
7	1,7	2,5	2,4	2,4	3,80	0,76	2,56
8	2,4	3,2	4,8	4,8	5,00	1,17	4,04
9	0,6	2,4	4,2	4,2	4,40	1,65	3,16
10	1,3	3,1	3,0	5,1	6,30	1,96	3,76

Fig. 31: Test results accuracy & Precision x-direction

Measurements Z-direction

Mass(g)	Measurements					Standard deviation	Average
50	1,2	1,4	1,2	1,3	1,5	0,13	1,32
150	3,1	3,1	3,6	3,1	3	0,24	3,18
200	6	6,4	6,5	6,9	6,9	0,38	6,54
300	7,7	8,2	9,1	8,3	8,6	0,52	8,38

Fig. 32: Test results accuracy & precision z-direction

APPENDIX H

CLIENT RESEARCH

In order to get an idea of the environment that our system needs to operate in, We have visited the zorgkwekerij Bloei at the Europalaan 16 in Pijnacker and greenhouse shop Lemuco in Delfgauw (figure 33). A list of questions and observations is made in table II and table III. The results have been used throughout our design process and requirement discovery. Both greenhouses have different applications. Lemuco focusses on crops while Zorgkwekerij Bloei focusses on flowers.



Fig. 33: Group Photo in Greenhouse

TABLE II: Questionnaire Zorgkwekerij Bloei

Questionnaire	Answer
What are nominal temperature ranges in your greenhouse?	15-30 degrees Celsius.
What are nominal humidity ranges in your greenhouse?	25-60%
Observed dirt	There is minor sand and leaves and sticks on the ground. Not too dirty.
What chemicals do you use?	We don't use any chemicals.
Any other needs you would like to see back?	A tool to get rid of weeds. Maybe a small weedwacker.

TABLE III: Questionnaire Lemuco

Questionnaire	Answer
What are nominal temperature ranges in your greenhouse?	15-45 degrees Celsius.
What are nominal humidity ranges in your greenhouse?	20-85%
Observed dirt	The robot would need to drive on the ground, so there is mud, sticks.
What chemicals do you use?	No chemicals are used.
Any other needs you would like to see back?	Weed laser system.

A. Client Research Conclusion

Both greenhouses see weeds as the most straining task for their employees and they both want a solution for this. This is outside of the scope of our project, but the parallel group will design a weedwhacking system. Both greenhouses don't use Chemicals, because they are a small company, they have more governmental restrictions. It's not worth to invest in chemicals for this reason they both said. Also sufficient data on the environments have been found in a greenhouse, except the UV-intensity of the sun.

APPENDIX I ANALYSIS

A. Finite Element Method

To gain insight into whether the components will withstand various forces and moments, a Finite Element Method (FEM) analysis was conducted. This analysis provides insight into stress concentrations and indicates if and where plastic deformations may occur. The FEM analyses were performed on 3 components (the tool adapter, robotarm adapter and the pin). In our view, these components experience the biggest loads and are most critical to the functioning of the tool-switching mechanism. The analysis was performed using the current material choice, PLA. See Figure 34 for the material properties associated with PLA that were used in the analysis.

First a note must be made about the reliability of FEM results on 3D printed parts. Since 3D prints do not have homogeneous

Property	Value	Units
Elastic Modulus	3500000000	N/m ²
Poisson's Ratio	0.35	N/A
Shear Modulus	2400000000	N/m ²
Mass Density	0.0013	kg/m ³
Tensile Strength	2700000	N/m ²
Compressive Strength		N/m ²
Yield Strength	26082000	N/m ²

Fig. 34: Material properties PLA

structures, the stress concentrations will distribute differently over the actual structure compared to what the FEM analysis suggests. Therefore, these FEM results provide more of an insight into the structure, and no design changes will be made based on these results. Only an analysis of the static forces on the mechanism was conducted, considering gravity and normal forces. In figure 35, 36, 37, and 38 the results are shown. Constraints are marked green, these are located at the heated inserts locations. The purple arrows are the normal forces which carry the weight of the tool adapter and tools. Finally the red arrow is gravity.

1) *Results:* The FEM analysis shows a maximum stress of $4.98 \times 10^4 N/m^2$ for the robotarm adapter and $7.18 \times 10^4 N/m^2$ for the tooladapter. The yield strength for PLA is $2.608 \times 10^7 N/m^2$, which is a factor of 1000 higher. Although this value is not fully reliable due to the different stress distributions in 3D printed PLA, the weakest points in the system can be identified from this FEM analysis. These weak points are located around the sharp edges of the V-shape and the holes for the heated insert.

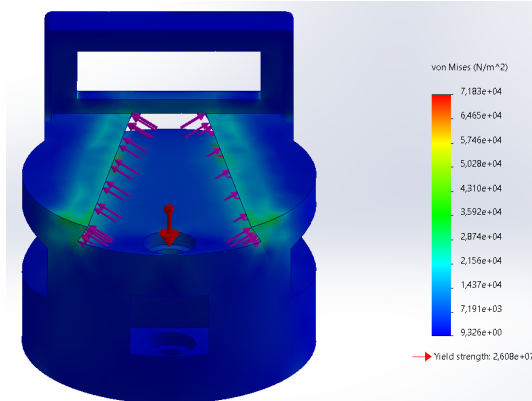


Fig. 35: FEM results tooladapter v-shape side

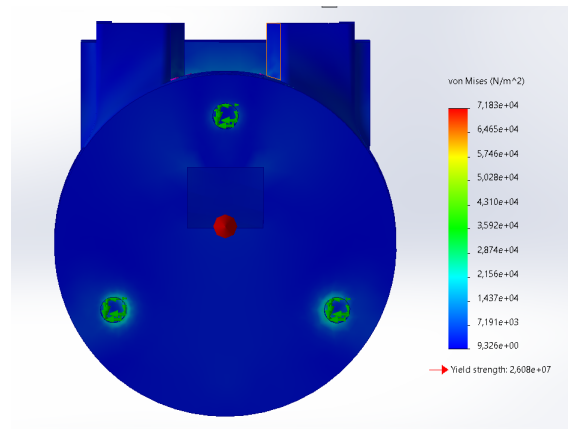


Fig. 36: FEM results tooladapter mounting side

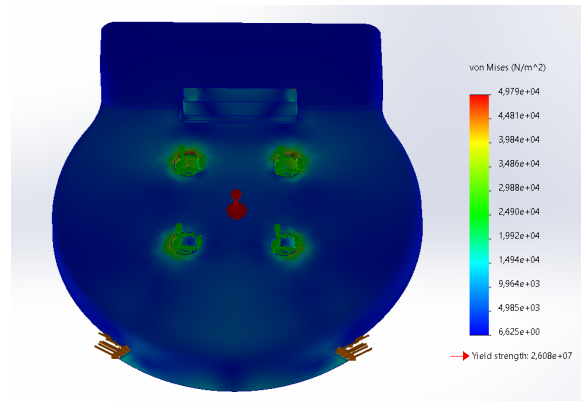


Fig. 37: FEM results robotarm adapter mounting side

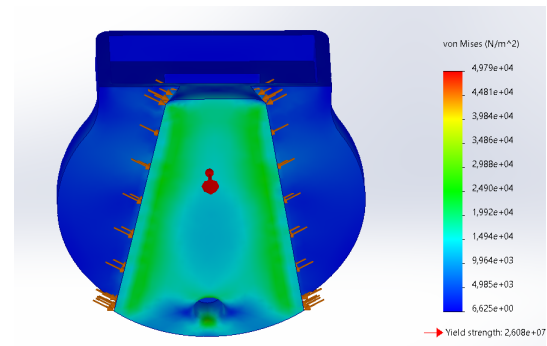


Fig. 38: FEM results robotarm adapter V-shape side

APPENDIX J CALCULATIONS

A. Magnets

For tight clamping between the tool holder and the tool adapter, magnets are used. The clamping force parallel to the walls of the tool holder is 15% of the perpendicular magnetic force specified in the material specifications of the magnet [2]. The perpendicular magnetic force is equal to $F_{magnet} = m \cdot g$. This becomes 11.8N (equation 2), based on the 1.2kg given in the specifications [16]. With two magnets on each side of the tool holder, a maximum parallel clamping force can be calculated (equation 3). Calculations for the magnets are depicted hereunder:

1) *Calculations magnets:*

$$F_{magnet} = m \cdot g = 1.2\text{kg} \cdot 9.81 \frac{\text{m}}{\text{s}^2} = 11.8\text{N} \quad (2)$$

With two magnets on each side of the tool holder, a maximum parallel clamping force can be calculated:

$$F_{magnets} = 2 \cdot 0.15 \cdot 11.8\text{N} = 3.5\text{N} \quad (3)$$

B. Spring

The spring constant has been calculated by the use of the elongation of the spring when the spring is loaded with a weight of 0.1kg. The spring has an unloaded length of 8.9mm and a loaded length of 9.4mm, which results in a spring constant k_{spring} of $1962 \frac{\text{N}}{\text{m}}$ (equation 4). When the tool adapter is placed in the tool holder, the spring is pressed 1.7mm. The friction coefficient of PLA is equal to 0.492 [8], which results in a friction force of 0.17N (equation 5). Together with the two parallel magnetic forces, the total force is equal to 3.67N. This force is larger than the 3.0N of the heaviest tool, which means that in the worst case scenario, the tool adapter can still fit the tool holder (equation 6). Calculations for the spring and the total force can be found hereunder:

1) *Calculations spring:* The constant of the spring becomes:

$$k_{spring} = \frac{F_{spring}}{u} = \frac{0.1\text{kg} \cdot 9.81 \frac{\text{m}}{\text{s}^2}}{(9.4 - 8.9) \cdot 10^{-3}\text{m}} = 1962 \frac{\text{N}}{\text{m}} \quad (4)$$

u is the elongation of the spring and F_{spring} is the force of the spring.

$$F_{friction} = \mu \cdot F_{spring} = 0.492 \cdot 1962 \frac{\text{N}}{\text{m}} \cdot 1.7 \cdot 10^{-3}\text{m} = 1.64\text{N}. \quad (5)$$

μ is the friction coefficient. The total force becomes:

$$F_{magnetic} + F_{friction} = 5.14\text{N} \quad (6)$$

APPENDIX K

PYTHON SCRIPTS FOR TESTS

A. Python script accuracy and precision X- direction

```

import rospy as rp
from geometry_msgs.msg import Pose, Vector3
from mirte_msgs.msg import *
from mirte_msgs.srv import *
from sensor_msgs.msg import *
from std_srvs.srv import *
import time
import math

#rosnodes
Base_angle=rp.ServiceProxy('/mirte/set_servoRot_servo_angle', SetServoAngle)
Shoulder_angle=rp.ServiceProxy('/mirte/set_servoShoulder_servo_angle', SetServoAngle)
Elbow_angle=rp.ServiceProxy('/mirte/set_servoElbow_servo_angle', SetServoAngle)
Wrist_angle=rp.ServiceProxy('/mirte/set_servoWrist_servo_angle', SetServoAngle)
GetPinValue = rp.ServiceProxy('/mirte/get_pin_value', GetPinValue)

#Coordinates
home = [[0, 0, 0,0]]
coordinate_51 = [[-1.05, -0.1888, 2.03, 1.087], [-1.05, -0.05, 2.012, 1.0835], [-1.05, -0.1888, 2.03, 1.087]]
coordinate_52 = [[-1.05, 0.2, 1.58, 1.188], [-1.05, 0.32, 1.58, 1.180],[-1.05, 0.2, 1.58, 1.188]]

coordinate_41 = [[-0.272, 0.6, 0.98, 1.448], [-0.272, 0.699, 0.98, 1.448], [-0.272, 0.6, 0.98, 1.448]]
coordinate_42 = [[-0.272, 1.1, 0.05, 1.77], [-0.272, 1.2, 0.05, 1.77], [-0.272, 1.1, 0.05, 1.77], [-0.272, 1.2, 0.05, 1.77]]

coordinate_31 = [[0, 0.50, 1.149, 1.36], [0, 0.60, 1.149, 1.36], [0, 0.50, 1.149, 1.36]]
coordinate_32 = [[0, 0.955, 0.32, 1.75], [0, 1.055, 0.32, 1.75], [0, 0.955, 0.32, 1.75]]

coordinate_21 = [[0.272, 0.6, 0.98, 1.448], [0.272, 0.699, 0.98, 1.448], [0.272, 0.6, 0.98, 1.448]]
coordinate_22 = [[0.272, 1.1, 0.05, 1.77], [0.272, 1.2, 0.05, 1.77], [0.272, 1.1, 0.05, 1.77], [0.272, 1.2, 0.05, 1.77]]

coordinate_11 = [[1.05, -0.1888, 2.03, 1.087], [1.05, -0.05, 2.012, 1.0835], [1.05, -0.1888, 2.03, 1.087]]
coordinate_12 = [[1.05, 0.2, 1.58, 1.188], [1.05, 0.32, 1.58, 1.180],[1.05, 0.2, 1.58, 1.188]]


def move_robot(coordinates):
    for item in coordinates:
        Base_angle(item[0])
        Shoulder_angle(item[1])
        Elbow_angle(item[2])
        Wrist_angle(item[3])
        time.sleep(1)

for i in range(5):
    move_robot(home)
    move_robot(coordinate_11)
    time.sleep(2)
    move_robot(coordinate_12)
    time.sleep(2)
    move_robot(coordinate_21)
    time.sleep(2)
    move_robot(coordinate_22)
    time.sleep(2)
    move_robot(coordinate_31)
    time.sleep(2)
    move_robot(coordinate_32)
    time.sleep(2)
    move_robot(coordinate_41)
    time.sleep(2)
    move_robot(coordinate_42)
    time.sleep(2)
    move_robot(coordinate_51)
    time.sleep(2)
    move_robot(coordinate_52)
    time.sleep(2)
    move_robot(home)

# #Movement

```

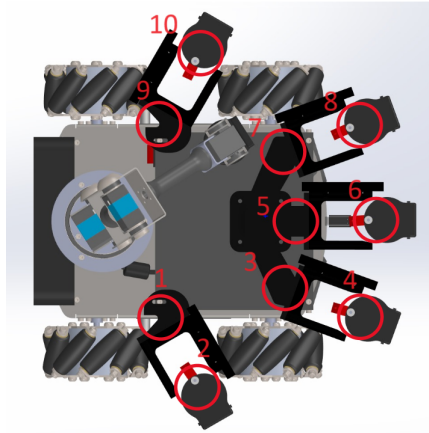


Fig. 39: Precision test ten different locations in the x-direction

B. Python script accuracy and precision Z- direction

```

import rospy as rp
from geometry_msgs.msg import Pose, Vector3
from mirte_msgs.msg import *
from mirte_msgs.srv import *
from sensor_msgs.msg import *
from std_srvs.srv import *
import time
import math

#rosnodes
Base_angle=rp.ServiceProxy('/mirte/set_servoRot_servo_angle', SetServoAngle)
Shoulder_angle=rp.ServiceProxy('/mirte/set_servoShoulder_servo_angle', SetServoAngle)
Elbow_angle=rp.ServiceProxy('/mirte/set_servoElbow_servo_angle', SetServoAngle)
Wrist_angle=rp.ServiceProxy('/mirte/set_servoWrist_servo_angle', SetServoAngle)
GetPinValue = rp.ServiceProxy('/mirte/get_pin_value', GetPinValue)

#Coordinates
home = [[0, 0, 0, 0]]
coordinate_1 = [[0, 0.21, 2.13, -0.826], [0, 0.285, 1.93, -0.73]]

#Toolholder 1

def move_robot(coordinates):
    for item in coordinates:
        Base_angle(item[0])
        Shoulder_angle(item[1])
        Elbow_angle(item[2])
        Wrist_angle(item[3])
        time.sleep(1)

    for i in range(5):
        move_robot(coordinate_1)

```

C. Python script repeatability test

```

import rospy as rp
from geometry_msgs.msg import Pose, Vector3
from mirte_msgs.msg import *
from mirte_msgs.srv import *
from sensor_msgs.msg import *
from std_srvs.srv import *
import time
import math

#rosnodes
Base_angle=rp.ServiceProxy('/mirte/set_servoRot_servo_angle', SetServoAngle)
Shoulder_angle=rp.ServiceProxy('/mirte/set_servoShoulder_servo_angle', SetServoAngle)
Elbow_angle=rp.ServiceProxy('/mirte/set_servoElbow_servo_angle', SetServoAngle)
Wrist_angle=rp.ServiceProxy('/mirte/set_servoWrist_servo_angle', SetServoAngle)
GetPinValue = rp.ServiceProxy('/mirte/get_pin_value', GetPinValue)

pinwaarde = GetPinValue('22','digital')

#Coordinates
home = [[0, 0, 0, 0]]

```

```

#Toolholder 1
Connecting_1 = [[1.05, 0, 0, 0], [1.05, -0.25, 2.21, 0.72], [1.05, 0.28, 2.09, 0.702], [1.05, 0.42, 1.85, 0.752], [1.05, 0.736, 1.27, 1.2]
Midway_1 = [1.05, 0.89, 0.726, 0]
Docking_1_heavy = [[1.05, 0.89, 0.726, 0], [1.05, 0.15, 0, 0], [1.05, 0.4, 0.8, 0.3], [1.05, 0.6, 1.22, 1.2], [1.05, 0.372, 1.85, 0.765]

#Toolholder 3
Connecting_3 =[[0, 0.15, 1.58, 0.757], [0, 0.678, 1.11, 1.255], [0, 0.81, 0.90, 1.30], [0, 1.126, 0.295, 1.57], [0, 1126, 0.295, 0]]
Docking_3_heavy = [[0, 0.4, 0, 0.4], [0, 0.8, 0.05, 1.5], [0, 0.98, 0.45, 1.53], [0, 0.448, 1.43, 1.176]]

#Toolholder 5
Connecting_5 = [[-1.05, 0, 0, 0],[-1.05, -0.25, 2.21, 0.72], [-1.05, 0.28, 2.09, 0.702], [-1.05, 0.42, 1.85, 0.752], [-1.05, 0.736, 1.27, 1.2]
Docking_5 = [[-1.05, 0.573, 1.48, 0.97], [-1.05, 0.46, 1.72, 0.878], [-1.05, 0.41, 1.87, 0.78], [-1.05, 0.23, 2.1, 0.757]]
Midway_5 = [-1.05, 0.89, 0.726, 0]
Docking_5_heavy = [[-1.05, 0.89, 0.726, 0], [-1.05, 0.15, 0, 0], [-1.05, 0.4, 0.8, 0.3], [-1.05, 0.6, 1.22, 1.2], [-1.05, 0.372, 1.85, 0.765]

runs = 0
succesfull_dockings = 0

def move_robot(coordinates):
    for item in coordinates:
        Base_angle(item[0])
        Shoulder_angle(item[1])
        Elbow_angle(item[2])
        Wrist_angle(item[3])
    time.sleep(1)

#Movement
for i in range(33):
    move_robot(Connecting_1)
    runs += 1
    if str(GetPinValue('22','digital'))[-1] == '1':
        succesfull_dockings += 1
    else:
        time.sleep(10)
    print(f"runs: {runs}, successful runs:{succesfull_dockings}")

move_robot(home)
move_robot(Docking_3_heavy)
move_robot(home)
move_robot(Connecting_3)
runs += 1
if str(GetPinValue('22','digital'))[-1] == '1':
    succesfull_dockings += 1

else:
    time.sleep(10)
print(f"runs: {runs}, successful runs:{succesfull_dockings}")

move_robot(home)
move_robot(Docking_5_heavy)
move_robot(Connecting_5)
runs += 1
if str(GetPinValue('22','digital'))[-1] == '1':
    succesfull_dockings += 1
else:
    time.sleep(10)

print(f"runs: {runs}, successful runs:{succesfull_dockings}")

move_robot(home)
move_robot(Docking_1_heavy)

print(f"runs: {runs}, successful runs:{succesfull_dockings}, finished!")

```

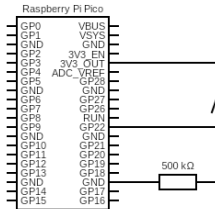


Fig. 40: Circuit diagram for measuring a connection with the tool adapter

APPENDIX L
TECHNICAL DRAWINGS

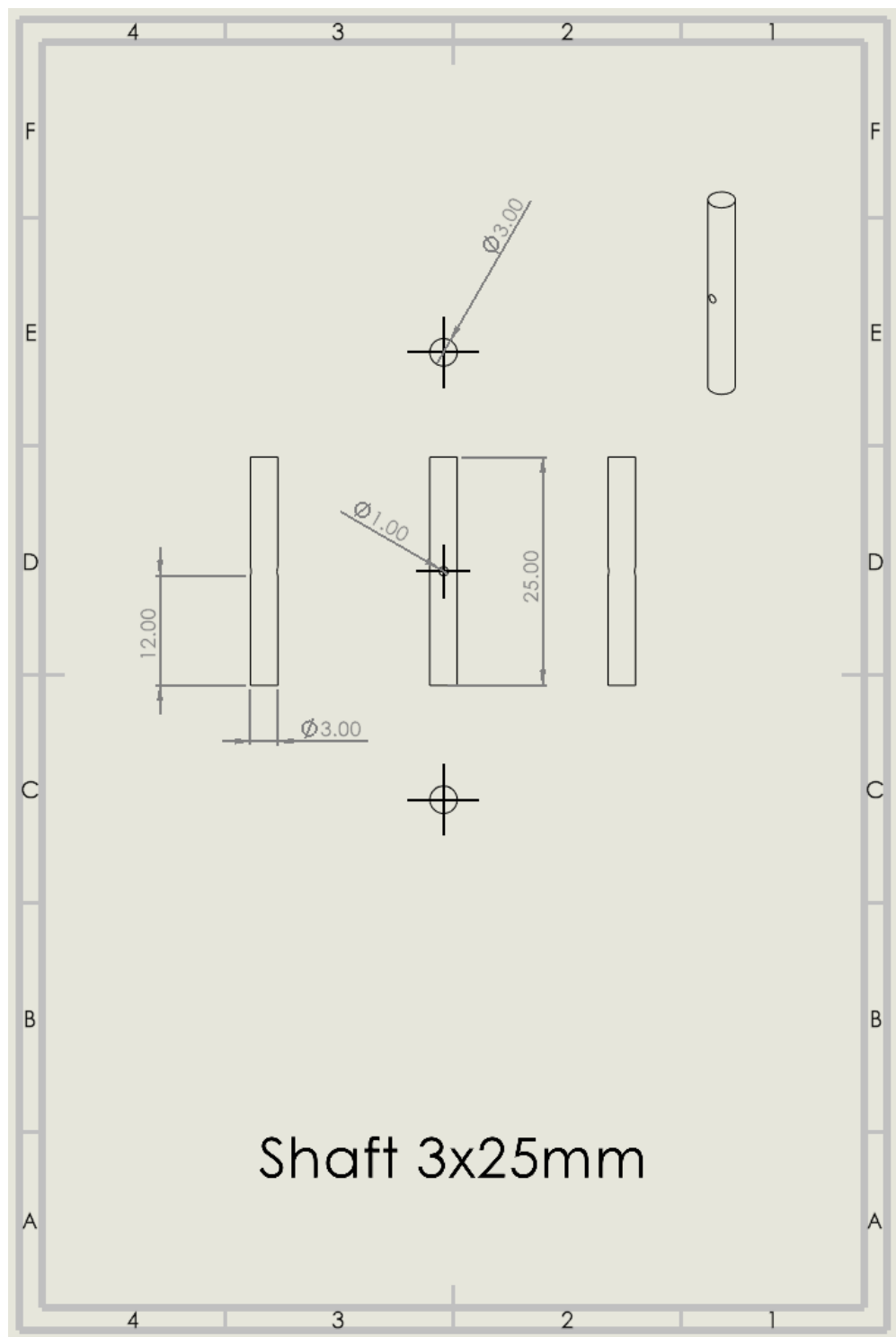


Fig. 41: Technical Drawing Shaft

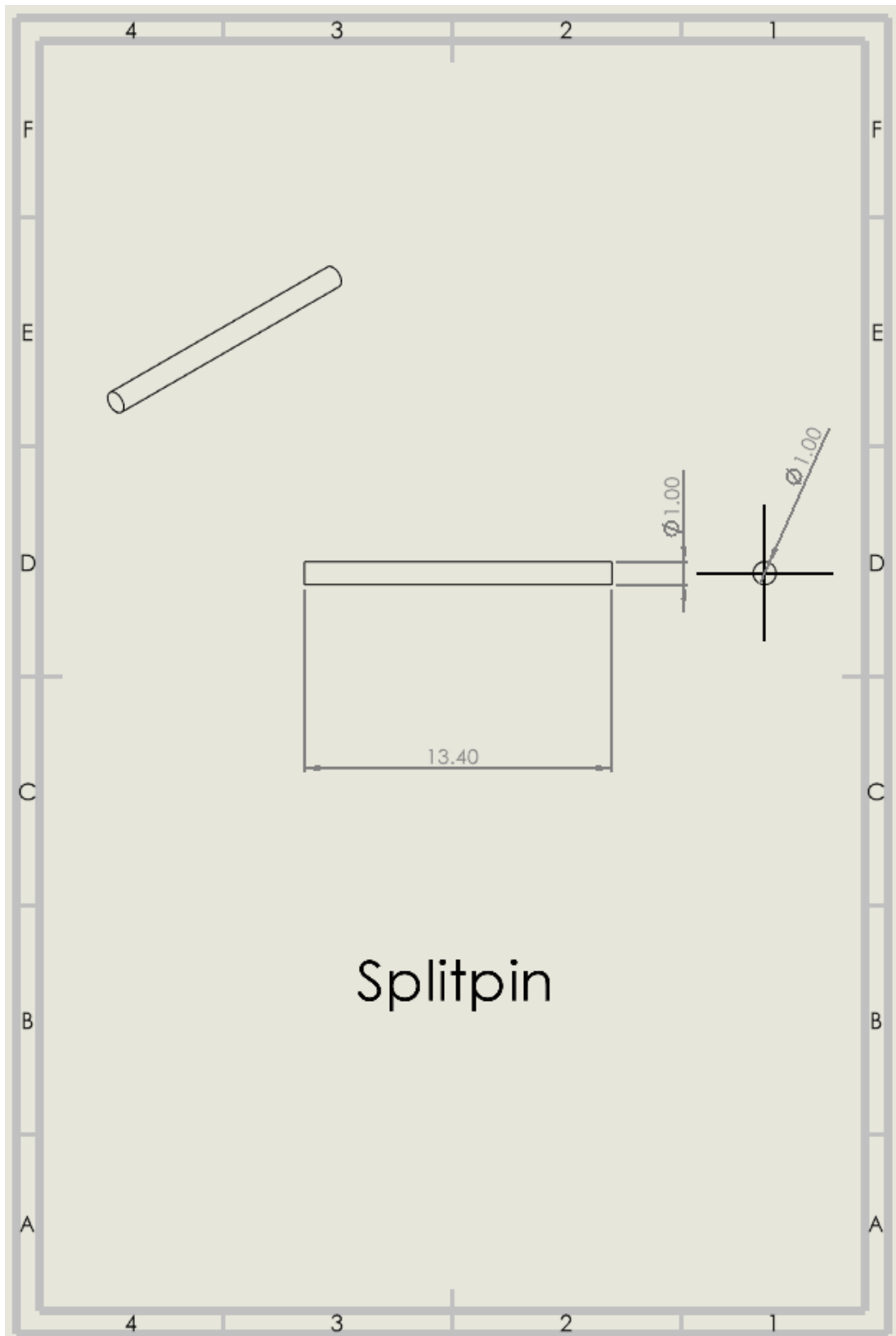


Fig. 42: Splitpin Technical Drawing

APPENDIX M

REQUIREMENT VERIFICATION MATRICES

	Verified
	Not Tested
	Not Verified

Fig. 43: Legend

1) **Test:** This entails the use of an end product to obtain the data needed to verify performance. It is the most resource intensive, so carefully thinking is necessary to determine what tests need to be conducted.

2) **Analysis:** This entails the use of mathematical modeling and analytical techniques to predict the suitability of a design to stakeholder expectations based on calculated data or data derived from lower system structure end product verifications such as a finite element analysis.

3) **Demonstration:** Showing that the use of an end product achieves the individual specified requirement. This can be done by taking a video of a certain action of the robot.

4) **Inspection:** The visual examination of the realized end product. Inspection is generally used to verify physical design features.

ID	Requirements	Parent	Compliance Method	Previous Design	Final Design
SR-01	The system shall cost less than 150 euros.	MNS	Inspection		
SR-02	The system shall be compatible with the Mirte Master.	MNS	Demonstration		
SR-03	The system shall be finished before the symposium.	MNS	Demonstration		
SR-04	The system shall be able switch tools within 10 [s].	MNS	Test		
SR-05	The system shall not damage the plants.	MNS	Demonstration		
SR-06	The system shall be as reliable as human beings.	MNS	Test		
SR-07	The system shall be able to operate in greenhouse conditions.	MNS	Test		
SR-08	The system shall be scalable.	MNS	Analysis		
SR-09	The system shall be maintainable.	MNS	Analysis		

Fig. 44: Stakeholder Requirements

ID	Requirements	Parent	Compliance Method	Previous Design	Final Design
FSR-01	The system shall couple 5 tools	MNS	Demonstration		
FSR-02	The system shall decouple 5 tools	MNS	Demonstration		
FSR-03	The system shall hold one tool at the time	MNS	Demonstration		
FSR-04	The system shall store 5 tools during operation	MNS	Demonstration		
FSR-05	The system shall be able to operate 5 different tools	MNS	Demonstration		

Fig. 45: Functional Requirements

ID	Requirement	Parent	Compliance Method	Previous Design	Final Design
SDR-01	The system shall have a mechanical connection between the arm and the tools.	[FSR-01][FSR-02] [FSR-03]	Inspection		
SDR-02	The system shall have an electrical connection between the arm and the tools.	[FSR-05]	Test		
SDR-03	The system shall provide space to store 5 tools	[FSR-04]	Demonstration		
SDR-04	The system shall be able to align with the tools	[FSR-01][FSR-02] [FSR-03][FSR-05]	Demonstration		

Fig. 46: Design Requirements

ID	Requirement	Parent	Compliance Method	Previous Design	Final Design
SPR-01	The system shall be able to mechanically connect/disconnect to 5 tools at least 1000 times.	[SDR-01][SR-06]	Test		
SPR-02	The system shall be able to electrically connect to 5 tools at least 1000 times.	[SDR-02][SR-06]	Test		
SPR-03	The system shall switch tools within a temperature range of 15 to 45 Celsius	[SDR-01][SDR-02][SR-07]	Analysis		
SPR-04	The system shall switch tools within a humidity range of 0% to 85%	[SDR-01][SDR-02][SDR-04][SR-07]	Test		
SPR-05	The system shall align with the tools within a precision of 5 mm in x- and z-direction	[SDR-01][SDR-02][SDR-04]	Test		
SPR-06	The system shall attach the tools within a precision/accuracy of [Mrite Masters accuracy] during the operation of the tools 1000 times.	[SDR-01][SDR-02]	Test		
SPR-07	The system shall be able to hold tools from 0 kg to 0.3 kg.	[SDR-01][SDR-02][SR-02]	Demonstration		
SPR-08	The system shall be able to operate for TBD times with TBD intensity of UV	[SR-07]	Analysis		

Fig. 47: Performance Requirements

APPENDIX N SCIENTIFIC SUBSTANTIATIONS

A. Scientific Substantiation Accuracy Hypothesis

When the mass is increased, the gravitational force F_g increases, which results in a greater moment $M = F \times r$ at greater distances, the moment around the arm increases. This has influence on the mechanic deformation of the arms and connection pieces that the endeffector is connected to, as well as the internal deformations of the internals of the servomotor that tries to withstand this moment. This deformation effect plays a big role in the z-direction accuracy of the arm. An estimation of the effect of the mass can be made of the effect of the mass and distance by separating these two main effects. To get an idea of the effects, we first look at a simplified worst case scenario where the servo motors are infinitely stiff, the arms are completely stretched and the force acting on the arms is perpendicular to the arm and that the material of the arms are solid PLA and is isotropic. A schematic depiction is provided in 48

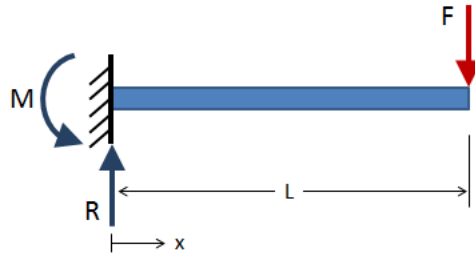


Fig. 48: Schematic overview worst case load on arm

The deformation of the endpoint is dependent on $F_g = m \cdot g$ [N] and the length L [m] from the endeffector to the origin, the elasticity modulus E [$\frac{N}{m^2}$] and the area moment of inertia I [m^4] and is given by equation 7.

$$\delta = \frac{F_g L^3}{3EI} \quad (7)$$

The arms of the Mirte Master are hollow cylindrical and the area moment of inertia is given by equation 8.

$$I = \frac{\pi}{64}(D^4 - d^4) \quad (8)$$

From these formulas, it can be concluded that for deformation, the higher the mass, the inaccuracy in z-direction scales linearly and the longer the distance from the rotation point, the inaccuracy in z-direction scales with a power of 3. From the specifications of the Mirte Master Solidworks model, the maximum length of the arms in stretched position is $L = 30\text{cm}$. Assuming a maximum weight of the tools of 300 grams. The maximum gravitational force would be $F_g \approx 3\text{N}$. Combined with $E_{\text{PLA}} = 3500\text{MPa}$ and $I \approx 10^{-7}\text{m}^4$ we get $\delta \approx 4 \cdot 10^{-5}\text{m}$ which is negligible in our case.

The second possibility is the internal deformation of the servomotors. The internals of a servo motor is in its simplest form a DC motor with gears. When assuming that arms are infinitely stiff and the DC motors do not fail under the load, any cause for inaccuracy at the endeffector would be caused by the deformation of the gears inside of the servo motor or the torsion displacement θ of the axis which the DC motor and the gears are connected to. The former is depicted in figure 50 and the latter is depicted in figure 49. The axis in figure 49 is the axis that connects the arm to the servo motor, this axis transmits

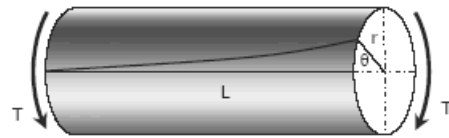


Fig. 49: Torsion of gear axe

all the force through the gears onto the DC motor's axis. This small axis is most prone to deformation as it directly transmits all the load onto gears with a high moment of inertia. So if the gears are assumed to be infinitely stiff, and for the worst case that that the tool with a maximum mass of 300 grams needs to be held at its maximum extended distance of $d = 30\text{cm}$ and that all of this moment goes to the shoulder servo, a moment of $T = m \cdot g \cdot d \approx 1\text{Nm}$ is generated around the axis of the connection point of the servomotor to the arm. Then the torsion deformation θ can be calculated with equation 9.

$$\theta = \frac{TL_{\text{as}}}{G_{\text{as}}I_{\text{as}}} \quad (9)$$

With $L_{as} = 0.01\text{m}$, $G_{as} = 80\text{GPa}$, $I_{as} \approx 10^{-11}\text{m}^4$ with a assumed diameter of a standard servomotor main axe of 2mm we find $\theta \approx 0.0159\text{rad}$. Over a distance of 30 cm this results in a displacement of 5mm. Which is as expected significantly larger than that of deformation. So it is known that the design parameters $z_3 - z_2 \geq 5\text{mm}$. Which we did and use for the test. Also from equation 9 It can be seen that the torsion displacement is linearly dependent on the torque T that is generated due to the mass and the distance of the tools. So for the total inaccuracy that is caused by torsion of the internal parts of the servo motor, it is expect to scale linearly with the mass m and distance d .

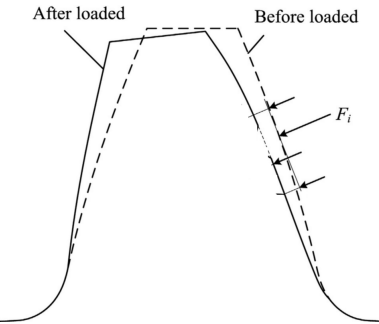


Fig. 50: Deformation of gear

The force F_i is the tangential force caused by the moment on the gear which is again cause by the mass at a certain distance.

Also the internal mechanical play of the servo gears play a role, but those plays can easily be measured by hand and cancel them out in our measurements as they are a systematic error.

B. Scientific Substantiation Precision Hypothesis

A heavier tool [kg] and a larger distance of the mass from the rotation point [cm] have the consequence that the servomotors need to generate more torque in order to compensate the gravity. This will result in more wear of the gears within the servomotors [14]. Subsequently, play (backlash) can take place, which is when there is too much distance between two adjacent teeth of a gear as depicted in figure 51. In this case, the small distance needs to be bridged first before the two teeth will touch each other [1]. Because of this, stochastic vibrations can occur, which decrease the precision [mm][6]. Play and thus stochastic vibrations can occur in all the three servomotors of which an overview is given in figure 52.

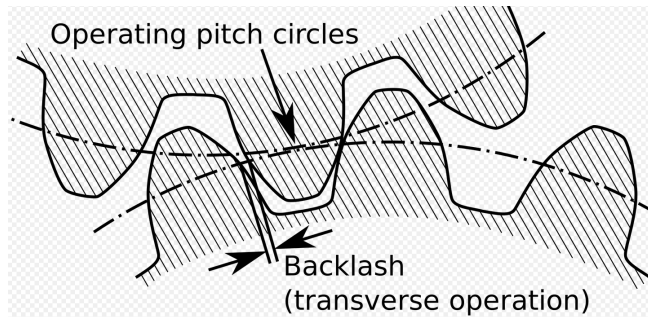


Fig. 51: Play (backlash) between two adjacent teeth [6]



Fig. 52: Schematic arm, with the servo's depicted in red

C. Scientific Substantiation Repeatability Hypothesis

Before the arm adapter connects to the pin, it first needs to slide over the upper surface of the pin so that the pin can fall into the hole on the upper surface of the pin. If the pin does not manage to fall into the hole, the connection fails. This can happen

if there is too much wear on the slope of the pin. The pin becomes then thinner and becomes more vulnerable for breaking. If the pin breaks, the pin can't stick beneath the tool holder anymore. A close-up of the pin has been depicted in figure 53.

A fundamental equation which describes wear, is Archard's wear equation. The wear thickness $h[m]$ can be calculated by equation 10 [14].

$$h = \frac{k \cdot F \cdot s}{A} \quad (10)$$

In this equation, $k[\frac{m^2}{N}]$ is the specific wear rate, a material dependant constant. $F[N]$ is the normal force, $s[m]$ the sliding distance and $A[m^2]$ is the contact area. It is assumed that the horizontal force generates $10N$ as seen in 53. This force is not exact, but it is on the order of the maximum weight of the applied tool. The angle of the pin is known, which is 45° , so the normal force F can be calculated with trigonometry relations (equation 11). Calculations can be seen in section J.

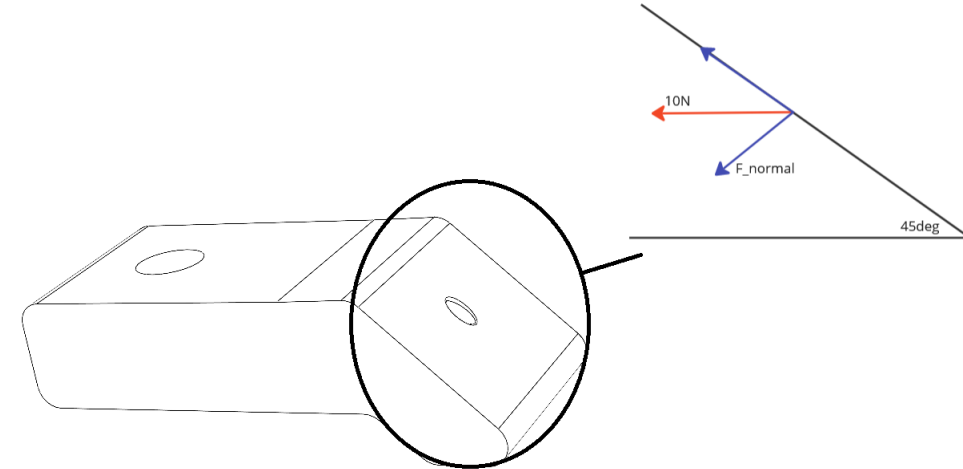


Fig. 53: Pin and force decomposition

The normal force has an order of $10^0 N$. If the mass increases, this force will increase as well, which would result in quicker wear and a smaller lifetime. The specific wear rate k is in the order of $10^{-15} \frac{m^2}{N}$ [14] and the sliding distance can be read from the SolidWorks model. The sliding distance has an order of $10^{-3} m$. The contact area has an order of $10^{-5} m^2$.

If the calculation is performed, the wear thickness of each slide is of the order of 10^{-13} (equation 12). Now it can be calculated that it takes approximately 10^{10} slides in order to lose $1mm$ of PLA due to wear (equation 13). In order to be on the safe side, the pin is made $1mm$ thicker than necessary. The pin will not break due to wear. Calculations are shown hereunder:

1) *Calculations of wear:* The normal force becomes:

$$F_{normal} = \cos(45) \cdot 10N = 5.3N \quad (11)$$

The wear per slide becomes:

$$h = \frac{10^{-15} \frac{m^2}{N} \cdot 10^0 N \cdot 10^{-3} m}{10^{-5} m^2} = 10^{-13} m \quad (12)$$

The number of slides to lose $1mm$ of thickness:

$$\frac{1mm}{10^{-10} mm} = 10^{10} slides \quad (13)$$

APPENDIX O

MATERIAL CHOICE

A. Introduction

For this project, the stakeholder requires the design to be operable in greenhouses SR-07. In order to comply to this requirement, the robot needs to be resistant against greenhouse conditions, such as UV-light, increased temperatures, humidity, and dirt (Requirements: SPR-08, SPR-03, SPR-04). In order to satisfy these requirements, the material of the robot needs to be chosen properly. However, our design will be attached to the Mirte Master and the Mirte Master is not ready to be deployed in greenhouses yet; our design will therefore not be tested in greenhouses. For this reason, it is decided that design criteria, such as stiffness and manufacturability is prioritized over weather resistance. The decision has been made to use PLA for our prototypes, but ASA as a recommendation for the use within greenhouses. However, still two greenhouses have been visited to check the actual circumstances in a greenhouse H and a conclusion has been reached that a high temperature and humidity are the main obstacles for a robot to operate properly in greenhouses. Underneath these influencing factors are explained and a short overview is given of how each factor could restrict the requirements of the robot. Also, designing recommendations are given.

B. Increased temperatures

From our client research during a visit to the greenhouses (Appendix H), it is found out that temperature ranges could range from 15 to 45 degrees. It is important to figure out if high temperatures could degrade the mechanical properties of our used material for the design to an extent where our functional requirement cannot be met (requirement SPR-03). A degradation of mechanical properties could lead to the failure of all functional requirements. High temperatures could cause a maximum volumetric expansion according to equation 14 [13].

$$\Delta A = 2 \times \alpha \times A_0 \times \Delta T \quad (14)$$

In this formula is the ΔA equal to the change of area, α equal to the expansion coefficient and the ΔT equal to the change of temperature and A_0 is the unexpanded surface area. An expansion could influence the accuracy and precision, and thus the docking of the robot arm adaptor to the pin FSR-01, FSR-02, FSR-03, FSR-04 and FSR-05. The expansion coefficient of PLA is $68 \frac{\mu m}{m^2 C}$ [12]. The total upper surface area of our tool holder has an area of $1294 \times 10^{-6} m^2$. During the visit to the greenhouses in Pijnacker H, it was found out that the maximum temperature difference is equal to $45^\circ C - 20^\circ C = 25^\circ C$. The new area becomes $0.0075 mm^2$ larger and this is negligible (equation 15). Therefore either the accuracy or the precision will not be changed due to a temperature change. Requirement SPR-03 is satisfied.

1) *Calculation maximum expansion:* The change in area at room temperature becomes:

$$\Delta A = 2 \times 68 \times 10^{-6} \times 2207 \times 10^{-6} m^2 \times 25^\circ C = 0.0075 mm^2 \quad (15)$$

C. Humidity

In greenhouses humidity ranges from 25 to 85 occur H. Humidity can have a negative impact on 3D printed filaments [5]. Some filaments are hygroscopic meaning that they absorb moisture from the air. Prolonged exposure to moist can cause problems. Expansion and shrinking can take place or degradation of the material. These can put the docking at risk and thus FSR-01, FSR-02, FSR-03, FSR-04 and FSR-05. PLA as a filament can not withstand prolonged humidity and therefore it should not be utilised in greenhouses. However, more humidity proof filaments exist (see Appendix O-E), so that requirement SPR-04 can be satisfied.

D. UV-light Resistance

UV-light plays an important factor regarding the growing of crops. However, too much UV-light can damage the material of the design. Chemical bonds can be destroyed, which has a degradation on the mechanical strength of the material and this could lead to failure of the robot FSR-05. The material needs to be UV-light resistant.

E. 3D Printer filaments

Hereunder, A setup of a comparison table with all possible filaments is made, which could be used for the design. It includes the print ability, weather resistance, heat resistance and the stiffness. According to this table, ASA (Acrylonitrile Styrene Acrylate) would be the best material option. It is weatherproof, stiff and heat resistant. It is applied for outdoor applications, for example garden furniture. It is a suitable material choice for tool switch robots operating in greenhouses.

Filament	Printable	Weatherproof	Heat resistant	Stiffness
PLA	Easy	Low (UV susceptible)	Low	High
PETG	Easy	Average	Good	Average
ABS	Medium	Low (UV susceptible)	Good	Average
ASA	Medium	Perfect	Good	Average
Nylon	Hard	Average	Perfect	High
Polycarbonaat	Average	Average	Perfect	Average

TABLE IV: Properties of different filaments [12]

APPENDIX P
STANDARD NORMAL DISTRIBUTION

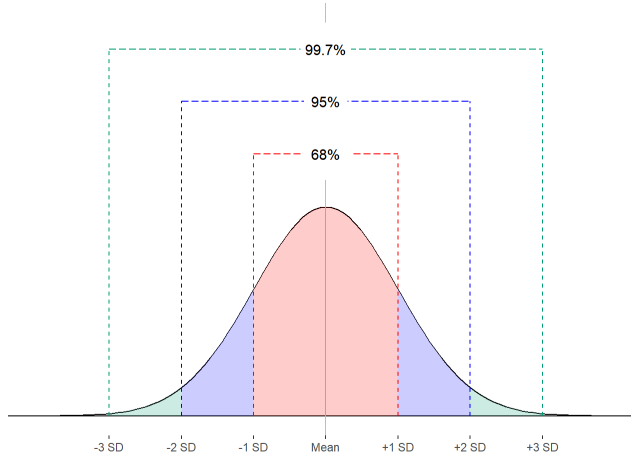


Fig. 54: Normal Distribution[4]